AMERICAN SOCIETY FOR MICROBIOLOGY | mBio®

RESEARCH ARTICLE
Ecological and Evolutionary Science

# The Origin, Succession, and Predicted Metabolism of Bacterial Communities Associated with Leaf Decomposition

**Sara L. Jackrel,[a]* Jack A. Gilbert,[b] J. Timothy Wootton[a]**

[a]Department of Ecology & Evolution, University of Chicago, Chicago, Illinois, USA
[b]Scripps Institution of Oceanography, University of California San Diego, La Jolla, California, USA

**ABSTRACT** Intraspecific variation in plant nutrient and defensive traits can regulate ecosystem-level processes, such as decomposition and transformation of plant carbon and nutrients. Understanding the regulatory mechanisms of ecosystem functions at local scales may facilitate predictions of the resistance and resilience of these functions to change. We evaluated how riverine bacterial community assembly and predicted gene content corresponded to decomposition rates of green leaf inputs from red alder trees into rivers of Washington State, USA. Previously, we documented accelerated decomposition rates for leaves originating from trees growing adjacent to the site of decomposition versus more distant locales, suggesting that microbes have a "home-field advantage" in decomposing local leaves. Here, we identified repeatable stages of bacterial succession, each defined by dominant taxa with predicted gene content associated with metabolic pathways relevant to the leaf characteristics and course of decomposition. "Home" leaves contained bacterial communities with distinct functional capacities to degrade aromatic compounds. Given known spatial variation of alder aromatics, this finding helps explain locally accelerated decomposition. Bacterial decomposer communities adjust to intraspecific variation in leaves at spatial scales of less than a kilometer, providing a mechanism for rapid response to changes in resources such as range shifts among plant genotypes. Such rapid responses among bacterial communities in turn may maintain high rates of carbon and nutrient cycling through aquatic ecosystems.

**IMPORTANCE** Community ecologists have traditionally treated individuals within a species as uniform, with individual-level biodiversity rarely considered as a regulator of community and ecosystem function. In our study system, we have documented clear evidence of within-species variation causing local ecosystem adaptation to fluxes across ecosystem boundaries. In this striking pattern of a "home-field advantage," leaves from individual trees tend to decompose most rapidly when immediately adjacent to their parent tree. Here, we merge community ecology experiments with microbiome approaches to describe how bacterial communities adjust to within-species variation in leaves over spatial scales of less than a kilometer. The results show that bacterial community compositional changes facilitate rapid ecosystem responses to environmental change, effectively maintaining high rates of carbon and nutrient cycling through ecosystems.

**KEYWORDS** bacterial metabolism, aquatic decomposition, ecosystem subsidies, intraspecific variation, environmental filtering, plant defensive chemistry, bacterial metabolism

Millions of years of coevolution between plants and their herbivores and pathogens have in part caused the diversity of plants we see today (1, 2). Plant chemical and mechanical defenses have played a critical role in this diversification, with over 200,000 described plant secondary metabolites that range from mild to high toxicity with an

**Citation** Jackrel SL, Gilbert JA, Wootton JT. 2019. The origin, succession, and predicted metabolism of bacterial communities associated with leaf decomposition. mBio 10:e01703-19. https://doi.org/10.1128/mBio.01703-19.

**Editor** Jennifer Martiny, University of California, Irvine



Address correspondence to Sara L. Jackrel, jackrel3@gmail.com.

* Present address: Sara L. Jackrel, Ecology, Behavior & Evolution Section, University of California San Diego, La Jolla, USA.

**Received** 28 June 2019
**Accepted** 9 August 2019
**Published** 3 September 2019

array of chemical structures with varied modes of action (3–5). Just as herbivores and pathogens have spurred plants to biosynthesize this diverse arsenal, bacteria have evolved to degrade these toxins. These bacteria, which may be either free-living decomposers of plants or symbiotic with an herbivore, have evolved diverse enzymatic pathways to degrade plant toxins with the benefit of unlocking this energy source (6). Bacterial detoxification and consumption of plant detritus are essential for maintaining the availability of carbon and nutrients for nonbacterial organisms within food webs (7).

While plants, herbivores, and bacteria have coevolved over long periods, the interactions among them are continually in flux. Evolution can occur over directly observable, ecological time frames, which has opened new questions about the roles of ecological versus evolutionary mechanisms in regulating ecosystem-level function (8). Bacteria in particular have short generation times. This could facilitate their rapid adjustment in the face of changing environmental conditions, such as changes in the distribution of plant resources, via either evolutionary or ecological mechanisms, such as environmental filtering.

In this study, we specifically evaluate the role of ecological mechanisms by investigating whether bacterial diversity, community composition, and gene content associated with metabolic pathways to breakdown plant secondary metabolites correspond to patterns of locally accelerated decomposition in a riverine system (9–11). Locally accelerated decomposition, or the "home-field advantage," in which decomposers more rapidly decompose leaves from trees of local origin, was originally documented by Gholz et al. (9). Further studies have shown the home-field advantage may be a widespread phenomenon, particularly in the soils of mature forests protected from most anthropogenic disturbances, where 77% of 35 studies demonstrated locally accelerated decomposition, with an average of 8% faster decomposition at Home locations (12, 13). More recently, the home-field advantage has been documented in aquatic systems where terrestrial leaf litter falls into rivers (14, 15). Further, this pattern has more recently been shown to also occur over small geographical scales of less than 1 km to individual trees within the same species (11). This local preference among aquatic and soil decomposers is driven in part by geographically variable secondary metabolites that are produced by plants to deter feeding by terrestrial herbivores (10). Such patterns of local acceleration could have arisen from either ecological or evolutionary mechanisms, including shifts in decomposer community composition, plasticity within decomposer individuals, or genetic change among populations of decomposers. To begin to unravel the underlying drivers of locally accelerated decomposition, we evaluate ecological mechanisms within bacteria.

We evaluate the role of bacteria as one component of the larger aquatic decomposer assemblage that includes fungi and invertebrates. Studies have found that leaf mass loss in stream systems is the consequence largely of invertebrates, followed by fungi and bacteria (16). However, taxonomic and functional databases of bacteria have been more thoroughly developed than those of fungi. Given the analytical tools currently available, we chose to focus on aquatic bacteria but note that fungi are key players in this ecosystem function. Additionally, although aquatic macroinvertebrates are important consumers of plant detritus in streams (17, 18), we previously found no evidence that aquatic invertebrates drove patterns of locally accelerated decomposition in streams because their abundance, taxonomic diversity, and functional diversity were similar among leaf packs of local versus nonlocal origin (14). A possibility that we do not investigate in this study is whether variation in aquatic macroinvertebrate gut microbiomes may drive locally accelerated leaf decomposition. We focus our study on the role of aquatic bacterial communities in driving locally accelerated leaf decomposition because of (i) the similar compositions of aquatic invertebrates despite differences in leaf decomposition; (ii) the ability of microbes to grow more rapidly, which would facilitate more fine-scale shifts in community composition in adjustment to plant traits; and (iii) the capacity of bacteria to detoxify plant secondary metabolites.

Here, we document the occurrence and successional patterns of free-living bacteria on red alder leaves derived from trees of local and nonlocal origin in a reciprocal green

leaf pack experiment completed in streams. We test our hypothesis that leaves of local origin will harbor a more specialized community of aquatic bacteria over the course of decomposition that is better able to rapidly break down the abundant local food source. Second, we test our hypothesis that the aquatic bacterial community inhabiting local leaves will undergo more rapid successional change than communities inhabiting leaves of nonlocal origin. For example, communities inhabiting local leaves might be more efficient at degrading secondary metabolites typical of a local site and therefore shift more rapidly to a community dominated by generalists that break down plant polysaccharides. In contrast, communities inhabiting nonlocal leaves may require a greater relative abundance and longer residence time of those bacterial taxa that are less efficient at metabolizing locally novel plant secondary compounds. For example, a greater relative abundance might occur if the degradation of these atypical metabolites requires multiple steps completed by more than one taxon whereas degradation of typical metabolites might require only a single taxon. Further, a longer residence time might be required if bacterial taxa which are not locally adapted are less efficient at degrading atypical metabolites and therefore do so at a lower rate. Overall, by evaluating differences in aquatic bacterial community composition, we provide insight into the potential mechanisms driving locally accelerated decomposition in streams, which may ultimately elucidate the tempo and trajectory of ecological changes within aquatic bacterial communities that confer locally beneficial function. Further, unraveling the underlying mechanisms of how bacteria might be adjusting to novel combinations of plant secondary metabolites may be pertinent for the field of bioremediation.

## RESULTS

Leaves of Home origin lost significantly more leaf mass by decomposition than leaves of Away origin (Fig. 1) (analysis of variance [ANOVA] ordered-heterogeneity test, $F_{4,68} = 1.8$; $r_sP_C$ statistic $= 0.75$; $P < 0.01$; see Materials and Methods for further description of the $r_sP_C$ statistic). Home leaves were those incubating at a site immediately downstream of their parent tree (i.e., Home as shown in Fig. S1 in the supplemental material), as well as those incubating at a site further downstream of the parent tree (i.e., "same river downstream" as shown in Fig. S1). Away leaves were those incubating at a site upstream of their parent tree (i.e., "same river upstream," as shown in Fig. S1), as well as those incubating at a different river from where their parent tree was growing (i.e., "away river" as shown in Fig. S1). This result of a significant home-field advantage was also consistent with findings using an alternative method that is more commonly used in terrestrial systems (13). For this alternative method, we used the subset of 20 leaf packs in our experiment that test for our main contrast across rivers, rather than Away sites within the same river (i.e., we used all leaf packs deployed on the "home site, on the home river" and one corresponding leaf pack on the Away river). We found Home leaves decomposed significantly more than Away leaves ($t_9 = 2.60$, $P = 0.029$, median home-field advantage index [HFAI] $= 44\%$; see the work of Ayres et al. [13] for details of HFAI calculation). Further, as previously reported by Jackrel et al. (10), the red alder trees used in this reciprocal transplant experiment differed significantly across the four riparian sites in their relative abundance of aromatic secondary metabolites, including ellagitannins and diarylheptanoids (see Fig. S2 for details). We therefore focus a portion of our analysis on bacterial metabolism of aromatic compounds.

We surveyed the bacterial community on leaves during decomposition as well as the bacterial community of the immediately surrounding environment to determine if the community composition corresponded with decomposition rate. The bacterial communities inhabiting the riparian soil, water column, terrestrial leaf, and aquatic leaf pack habitats each formed significantly distinct clusters from each other habitat in principal-coordinate space, when considering either the relative abundance-weighted or unweighted phylogenetically based community distance metric, UniFrac (Fig. S3; all pairwise analysis of similarity [ANOSIM] $P < 0.01$) (19). Using the Bayesian tool Source-

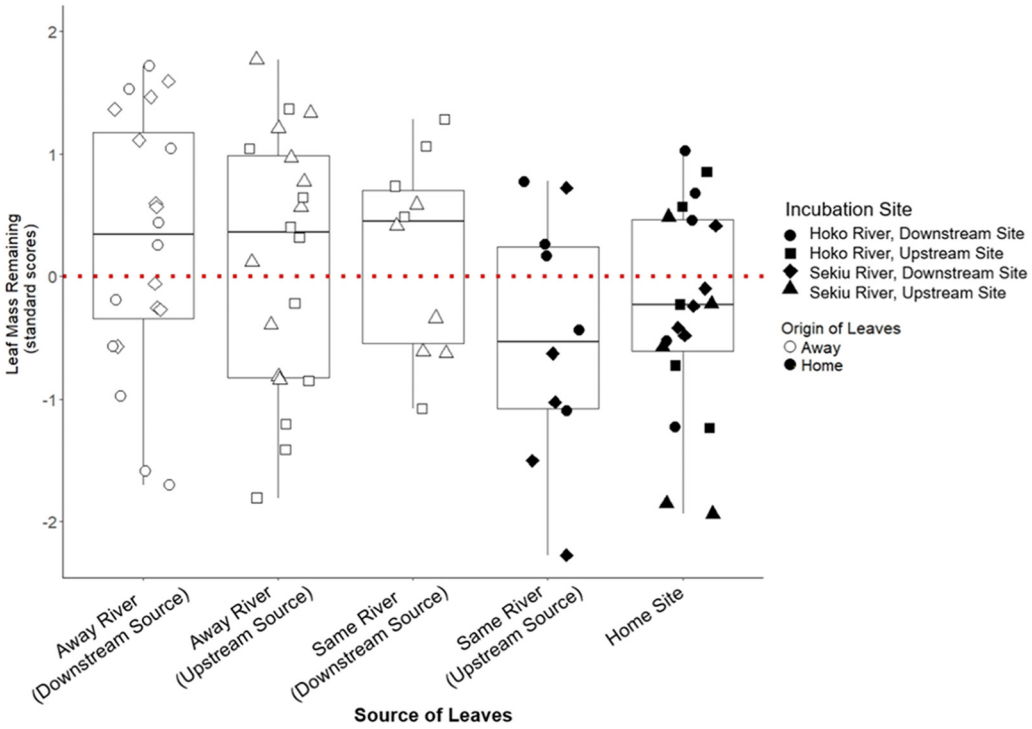


**FIG 1** Decomposition measures of leaves from 20 riparian red alder trees used in a reciprocal transplant experiment across the Hoko and Sekiu Rivers, WA, USA. Leaves of local origin decomposed significantly faster than leaves from trees growing in locations that would not naturally reach the incubation site, including trees growing along the same river but downstream of the incubation site and trees growing at the other river. Note that the *y* axis depicts decomposition rates as standardized scores (i.e., *z*-scores), in which decomposition rates within an incubation site are adjusted to $\mu = 0$, SD = 1, so a *y* axis value = 1 indicates 1 SD above the mean decomposition rate at that incubation site. For example, the standardized score for a leaf pack, referred to as "pack 1," incubating at the Hoko River, Downstream Site would equal (% mass loss of pack 1 at Hoko, Downstream − mean % mass loss of all packs incubating at Hoko, Downstream)/(standard deviation of % mass loss of all packs incubating at Hoko, Downstream). This standardization serves to illustrate the relative decomposition rates of Home versus Away leaves at each site rather than variation among sites; however, our mixed-effects model was run on the nonstandardized decomposition data with incubation site as a random effect term (leaf origin term: $F_{4,68} = 2.6$, $r_s P_C = 0.3$, $P = 0.01$). For nonstandardized data, see Fig. S8. Categories on the *x* axis include, from right to left, trees growing immediately upstream of the incubation site and trees growing further upstream of that incubation site at the "Away Site" on the same river, both of which are considered "Home," and then trees growing downstream of the incubation site at the "Away Site" on the same river, trees growing at the upstream site on the paired river, and trees growing at the downstream site on the paired river, all three of which are considered "Away." Note that all points are horizontally jittered to minimize overplotting.

Tracker to predict the potential source of bacterial operational taxonomic units (OTUs) associated with each aquatic leaf pack, we found that aquatic bacterial communities on leaves were derived more from terrestrial leaves (66.7% ± 0.86% [standard error {SE}]) and unknown sources (29.6% ± 0.89%), while bacteria sourced from riparian soil and the river water column contributed marginally (0.82% ± 0.039% and 2.9% ± 0.14%, respectively) (20). These proportions varied considerably over time and by whether the leaves originated from Home or from Away sites; however, these results were site dependent as indicated by a significant day × leaf origin × site interaction in an analysis of variance ($F_{5,290} = 4.3$, $P < 0.001$ [Fig. 2A and B]). The proportion of bacteria from taxa that were sourced from terrestrial leaves tended to increase over the course of the experiment from an average of 59.0% ± 2.2% during day 5 to an average of 74.2% ± 0.7% during day 20 (ANOVA: $F_{1,290} = 11.7$, $P < 0.001$ [Fig. S4A and B]).

The greatest contributor to differences in bacterial community $\beta$-diversity was the river in which the leaf packs were incubated when considering a relative abundance-unweighted phylogenetic metric (Fig. 2A). In contrast, succession was the greatest contributor to $\beta$-diversity differences when considering either a relative abundance-weighted phylogenetic metric (Fig. 2B) or a nonphylogenetic metric (Fig. 2C). These contrasting results indicate that habitat location is the primary driver of OTU presence/

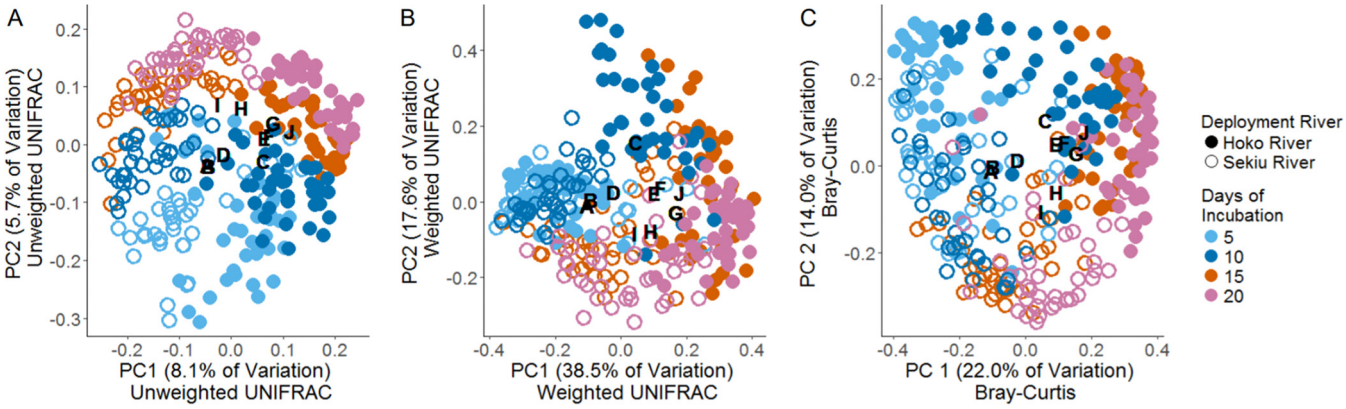


**FIG 2** Successional changes among the aquatic bacterial community inhabiting and decomposing leaves from riparian red alder trees deployed in leaf packs on the streambeds of the Hoko and Sekiu Rivers, WA, USA. Community similarity is depicted using principal-coordinate analyses of either relative-abundance unweighted (A) or weighted (B) phylogenetic distance using the UniFrac metric, as well as the non-phylogenetically based Bray-Curtis distance metric (C). A biplot analysis depicts where the 10 most abundant taxa for all leaf pack samples, labeled taxa A to J, occur in principal-coordinate space to visualize successional changes among taxa. The earliest stage of decomposition, during day 5, is characterized by high relative abundance of taxa A and B, both in the order *Burkholderiales*, family *Comamonadaceae*. Mid-stage decomposition, during days 10 and 15, is characterized by increased relative abundance of taxa C (order *Myxococcales*), D (order *Sphingomonadales*, family *Sphingomonadaceae*, genus *Novosphingobium*), E (order *Rhodobacterales*, family *Rhodobacteraceae*, and genus *Rhodobacter*), and F (order *Sphingomonadales* and family *Sphingomonadaceae*). The last stage of decomposition, during day 20, was characterized by a high relative abundance of taxa G (order *Cytophagales*, family *Cytophagaceae*, genus *Flectobacillus*), H (order *Flavobacteriales*, family *Flavobacteriaceae*, genus *Flavobacterium*), I (order *Rhizobiales*, family *Rhizobiaceae*, and genus *Agrobacterium*), and J (order *Rhizobiales*).

absence, whereas successional stage is the primary driver of OTU relative abundance. Metrics incorporating relative abundance are usually more representative of community function; however, see the work of Jousset et al. (21) for a review of the potentially disproportionate role of rare taxa in ecosystem function. The Hoko River was characterized by a high relative abundance of taxa in the orders *Rhizobiales*, *Cytophagales* (family *Cytophagaceae*, genus *Flectobacillus*), *Sphingomonadales* (family *Sphingomonadaceae*), *Rhodobacter* (family *Rhodobacteraceae*, genus *Rhodobacter*), and *Myxococcales*. The Sekiu River was characterized by a high relative abundance of taxa in the orders *Burkholderiales* (family *Comamonadaceae*) and *Rhizobiales* (family *Rhizobiaceae*, genus *Agrobacterium*).

Early-stage decomposition was characterized by a very high relative abundance of taxa in the order *Burkholderiales* (family *Comamonadaceae*) (ANOVAs: taxon relative abundance predicted by day, all $P < 0.001$; see Fig. S5). OTUs in this family typically comprised over 50% of the early-stage community (Fig. S3). Mid-stage decomposition during days 10 and 15 was characterized by increased relative abundance of bacteria in the orders *Myxococcales*, *Sphingomonadales* (family *Sphingomonadaceae*, genus *Novosphingobium*), and *Rhodobacterales* (family *Rhodobacteraceae*, genus *Rhodobacter*) ($P < 0.001$ for all ANOVAs [Fig. S5]). Late-stage decomposition during day 20 was characterized by an increased relative abundance of taxa belonging to the orders *Cytophagales* (family *Cytophagaceae*, genus *Flectobacillus*), *Flavobacteriales* (family *Flavobacteriaceae*, genus *Flavobacterium*), and *Rhizobiales* (family *Rhizobiaceae*, genus *Agrobacterium*) ($P < 0.001$ for all ANOVAs [Fig. S5]). We provide a full list of taxa that change significantly in relative abundance over time in Fig. S5 where we categorize taxa as characteristic of early-, mid-, or late-successional communities based on visual inspection of relative abundance plots ($P < 0.05$ for all ANOVAs of taxon relative abundance predicted by day; see Fig. S5). We also separately list taxa with significant, but site-dependent, successional patterns that may be hypothesized to play a larger role in driving locally accelerated decomposition patterns (Fig. S5). Many of the taxa that became quite abundant in leaf packs during the later stages of decomposition remained exceedingly rare at less than 0.01% of the water column community (Fig. S3). We also found that leaves of Away origin were inhabited by communities richer in $\alpha$-diversity than leaves of Home origin and that this difference in Faith's phylogenetic diversity (PD) by leaf origin was consistent throughout stages of decomposition (Fig. S6,

ANOVA: leaf origin, $F_{1,315} = 2.39$, ordered *a priori* $r_sP_C < 0.01$). Further, alpha-diversity varied by site (ANOVA: site, $F_{3,315} = 1{,}942.5$, $P < 0.001$) but remained stable over the course of succession (ANOVA: day, $F_{1,315} = 0.30$, not significant [NS]).

We next analyzed changes in the predicted metabolic functional capacity of bacterial communities both over succession (i.e., day) and by leaf origin. Our predicted metagenome functions are derived from bacterial taxa with reasonably short evolutionary distances to yield accurate predictions (average nearest sequences taxon index $< 0.10$, validated by Langille et al. [22]). Bacterial communities that inhabited leaves during the earliest stage of decomposition had the greatest predicted capacity to degrade aromatic compounds, with a significant decline in predicted capacity through succession (Fig. 3A) ($R^2 = 0.33$, $P < 0.001$, gene content predictions for day 5 = 21,566 ± 365 [mean ± SE], day 10 = 19,826 ± 497, day 15 = 17,702 ± 365, day 20 = 15,284 ± 187). During the earliest stage of decomposition, day 5, when the relative abundance of these taxa was greatest, we found that communities inhabiting leaves of Away origin contained a greater proportion of these taxa than communities inhabiting leaves of Home origin (Fig. 3B) (ANOVA: leaf origin, $F_{1,52} = 32.6$, $P < 0.001$). Further, Home versus Away leaf origin predicted the relative abundance of 12 molecular functional terms within the aromatic degradation pathway (ANOVA: leaf origin, all $P$ values $< 0.05$ after false-discovery rate correction for multiple comparisons). For an illustration of the role that each of these 12 molecular functional terms play within this pathway, see Fig. S7. We found that the bacterial communities inhabiting leaves of Home versus Away origin differed significantly in the predicted relative abundance of a mixture of enzymes required for degrading aromatic compounds (Fig. 3C). The more abundant taxa predicted to be capable of degrading aromatic compounds that contributed most toward these functional measures belonged to two families, the *Comamonadaceae*, which contributed 45.3% summed across all leaf samples of gene content corresponding to aromatic degradation and *Sphingomonadaceae*, which contributed 31.0%. Other families that contributed substantially to these predicted functions were *Oxalobacteraceae* (3.5%), *Rhizobiaceae* (3.4%), *Rhodobacteraceae* (3.2%), *Caulobacteraceae* (1.7%), *Phyllobacteriaceae* (1.2%), *Hyphomicrobiaceae* (1.1%), *Neisseriaceae* (1.1%), and *Cytophagaceae* (1.1%). An additional 49 families contributed less than 1.0% toward the total predicted gene content for aromatic degradation.

In addition to focusing specifically on leaf secondary metabolites, we also evaluated the effect of succession (i.e., day) and leaf origin on the more general degradation of leaf material. As decomposition progressed, the bacterial community became increasingly dominated by taxa with the predicted functional capacities categorized in the "metabolism of starch and sucrose" pathway ($R^2 = 0.27$, $P < 0.001$ [Fig. 4A; see Fig. S7 for specific molecular functional terms included in this pathway]). This diverse pathway includes the enzymes known to degrade the plant polysaccharide cellulose, including endoglucanase (K01179) and cellulose 1,4-beta-cellobiosidase (CBH1) (K01225). In addition to this broader category of "metabolism of starch and sucrose," we highlight five specific molecular functional terms implicated in cellulose degradation that increased significantly over succession (Fig. 4B to F). However, during the final stages of decomposition, day 20, we did not find differences in the starch and sucrose predicted metabolic capacities of bacteria inhabiting leaves of Home versus Away origin, either when summing function across the entire pathway (Fig. 4G) or in our cellulose-specific pathway of these five molecular functional terms (Fig. 4H).

Last, we aimed to determine an adequate minimal model for predicting the rate of leaf decomposition by considering the relative importance of leaf bacterial diversity, bacterial predicted metabolic function, and our leaf origin treatment. Considering evidence that biological diversity often promotes ecosystem functions (23), we hypothesized Faith's phylogenetic diversity (24) might promote more rapid leaf decomposition. Further, we included the second two terms in the model because plant defense compounds are thought to be toxic and/or repellent toward decomposers as a means of preventing decomposition of nondefended components of the plant tissue. Therefore, we hypothesized that rapid decomposition may occur among local leaves with

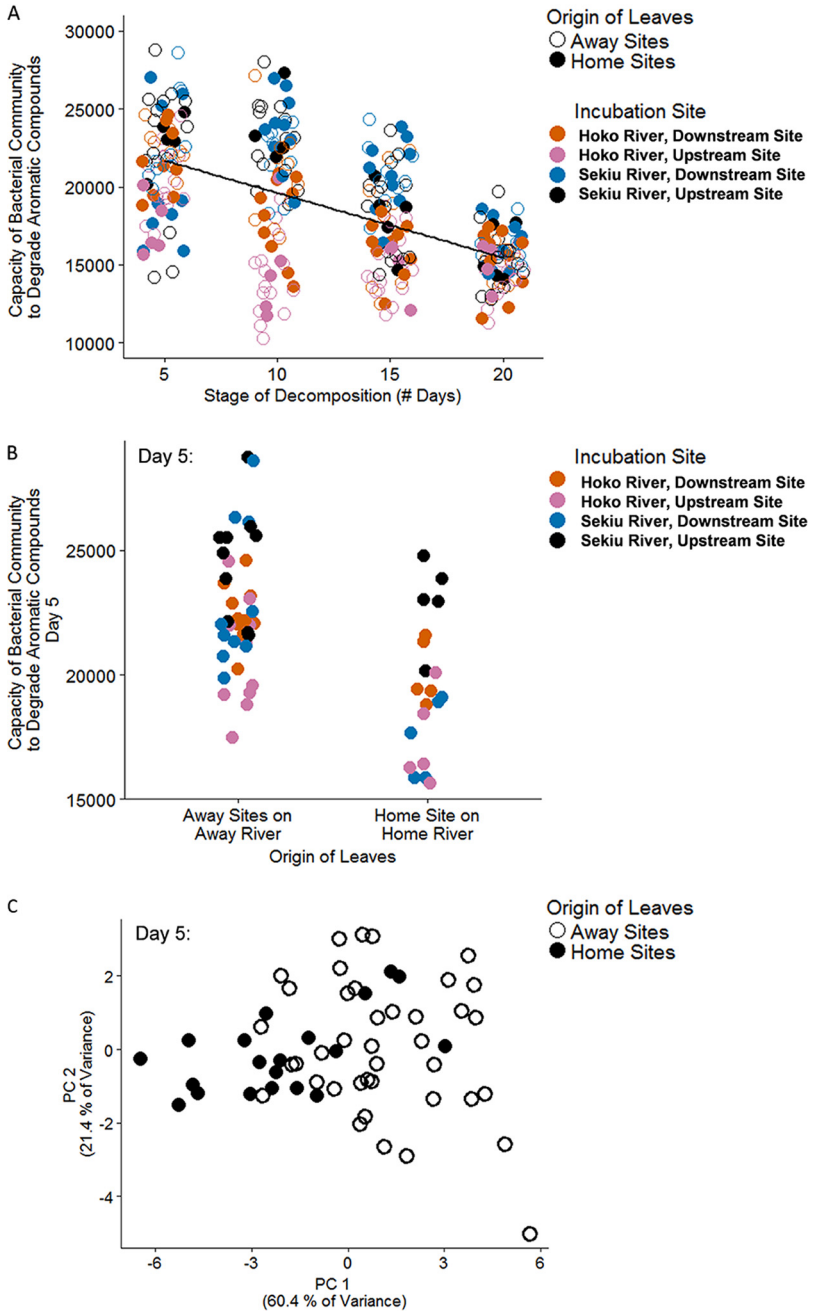


**FIG 3** (A) Decline in predicted aromatic degradation ability of the bacterial community during leaf succession ($F_{1,157} = 313$, $P < 0.001$, $R^2 = 0.33$). (B) Differences of ability as a function of leaf source and incubation locations early in succession (ANOVA: site $F_{3,52} = 11.8$, $P < 0.001$; leaf origin $F_{1,52} = 32.6$, $P < 0.001$). Note that for panels A and B, *y* axis units are gene content predictions as calculated via PICRUSt, and points are horizontally jittered to minimize overplotting. (C) In addition to differences in the summed capacity to degrade aromatics, early-successional bacterial communities (i.e., day 5) differed as a function of leaf origin in the relative abundance of different enzymes that contribute to the summed capacity to degrade aromatic ring structures. We defined "summed capacity" as that of all KEGG terms included in the pathway that were represented in our data set to obtain a total measure of pathway function per sample. Figure S7 gives principal-coordinate (PC) axis loadings. Note that panel A included all leaf origin categories, whereas panels B and C consider only the strongest contrast: Home Site on the Home River versus Away River sites.

specialized bacterial communities predicted to have a relatively high capacity to degrade aromatics in early stages of decomposition, followed by communities predicted to have a high capacity to degrade cellulose during later stages of decomposition. We found that the phylogenetic diversity and predicted functional composition of

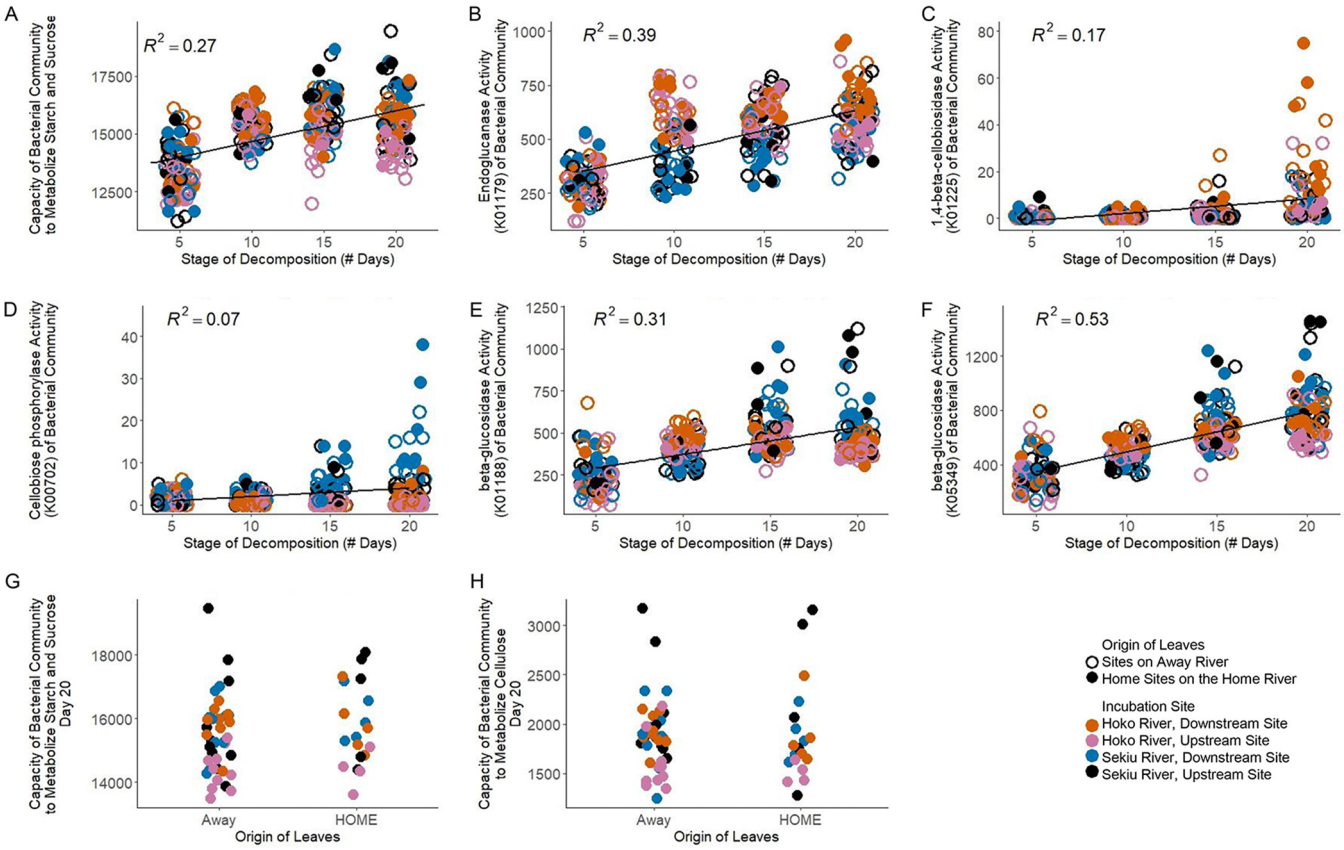


**FIG 4** Successional patterns of starch and sucrose metabolism pathways in the bacterial community. (A) Overall predicted functional capacities from all molecular functional terms, including enzymes known to degrade the plant polysaccharide cellulose, such as endoglucanase and cellulose 1,4-beta-cellobiosidase increase over time $F_{1,313} = 120.6$, $P < 0.001$. (B to F) Prevalence of 5 enzymes involved in cellulose breakdown that increase significantly with succession. (G and H) Total predicted functional capacity to degrade starch and sucrose (G) and total predicted functional capacity to degrade cellulose (H) do not vary as a function of leaf origin during the latest stage of leaf decomposition, day 20. Note that panels A to F included all leaf origin categories, whereas panels G and H considered only the strongest contrast: Home Site on the Home River versus Away River sites. Also note that all *y* axis units are gene content predictions as calculated via PICRUSt, and all points are horizontally jittered to minimize overplotting.

the bacterial community were significantly predictive of the rate of leaf decomposition (Faith's PD $F_{1,8} = 3.3$, predicted cellulose degradation $F_{1,8} = 1.0$, predicted aromatic degradation $F_{1,8} = 6.7$, marginal $R^2 = 0.057$). This model incorporating bacterial diversity and predicted functional patterns explains nearly as much variance as a model including our leaf origin treatment as the sole predictor of decomposition rate (leaf origin $F_{4,9} = 14.7$, marginal $R^2 = 0.064$). The leaf origin model fit the data significantly better than the bacterial model, as determined with a log-likelihood test of Akaike information criterion (AIC) scores. However, considering all measures together generated the best-fitting model; adding our metrics of bacterial alpha-diversity and metabolic function significantly improved the leaf origin model (leaf origin $F_{4,12} = 15.0$, Faith's PD $F_{1,8} = 4.3$, predicted cellulose degradation $F_{1,8} = 1.3$, predicted aromatic degradation $F_{1,8} = 3.2$, marginal $R^2 = 0.15$). We also used a second approach to determine the relative importance of bacterial diversity, predicted functional metabolism, and leaf origin on decomposition rate. We summarized our predictor variables as principal components and used these principal components in a model as composite variables predictive of decomposition rate. These results generated similar conclusions that leaf origin is a stronger predictor of decomposition rate than bacterial measures, but bacterial community composition further improves prediction in the final model (PC2 with loadings on bacterial predicted functional metabolism $F_{1,311} = 13.5$; PC3 with loadings on leaf origin $F_{1,311} = 28.5$ [Table S1]).

## DISCUSSION

Our results suggest that we can begin to characterize the role of particular freshwater bacterial taxa in degrading allochthonous leaf litter in streams. We found similar patterns of successional change across leaf packs from multiple trees in each of our two study rivers. A core generality emerged from the patterns of succession that we documented: microbial taxa specialized in breaking down aromatic secondary metabolites of leaves dominated early stages of succession, whereas taxa that efficiently break down more generalized plant tissue components, such as cellulose and starches, dominate later stages. Studies of microbial decomposition of both plants and animals increasingly find clearly defined stages of microbial succession (25–28). For example, bacterial succession on mammalian corpses is sufficiently consistent across environments to warrant use of the microbial community for forensic predictions (26). We found that the most relatively abundant taxa during each stage of decomposition tended to be rare in the water column, which agrees with previous findings that key taxa involved in animal decomposition are initially exceedingly rare but widespread in terrestrial soils across environments (26). Succession was the primary source of variation among freshwater bacterial communities when weighting by relative abundance of each taxon. However, the river during incubation was the primary source of variation when considering non-relative-abundance-weighted communities. Regardless of using a weighted or nonweighted metric of relative abundance, leaf origin was responsible for a smaller, yet statistically significant, proportion of the variation among bacterial communities. Prior studies of the freshwater microbial communities inhabiting leaves from different genotypes of cottonwood trees also found that the environment was a more substantial driver of community variation than leaf traits (29).

Beyond expanding our understanding of bacterial successional patterns that drive decomposition of leaves in rivers, we find evidence of the mechanisms by which freshwater bacteria may be accelerating the decomposition of local leaves. Specifically, this evidence supports our first hypothesis that leaves of local origin will harbor a more specialized community of aquatic bacteria over the course of decomposition that is better able to rapidly break down the abundant local food source. Leaf secondary metabolites, which are often toxins targeting herbivores and microbial enemies (30, 31), vary among the *Alnus rubra* trees studied here. Although not necessarily targeting decomposing microbes, these toxins must nonetheless be neutralized before the nontoxic leaf components are accessible to the broader microbial and invertebrate decomposer community. We found that during early succession, leaves derived from local versus nonlocal trees were inhabited by significantly different communities. It is intuitive that we would find our most striking differences between Home and Away leaves at the earliest stages of decomposition because while leaf secondary metabolites are diverse and structurally complex, they are constructed of many of the same building blocks that ultimately degrade to a small number of simple sugars that are accessible to many microbial taxa (however, it should be noted that studies have also shown that the magnitude of differences between Home and Away leaves may increase over the course of decomposition in some terrestrial environments [32]). During the earliest stage of decomposition, freshwater bacterial inhabitants are likely to be specialists capable of degrading intact secondary metabolites that we have shown to vary spatially in relative abundance across this landscape (see Fig. S2 in the supplemental material) as well as other aromatic compounds such as lignin. Predicted functional annotation revealed that leaves were inhabited early by taxa capable of degrading aromatic compounds and that this metabolic capacity to degrade aromatic compounds differed between Home and Away leaves. We therefore infer that these taxa are involved in locally accelerating decomposition. We base this inference on our prior work showing that Home and Away leaves differ in their composition of aromatic compounds and that these differences drive leaf decomposition rates (10). Further supporting our first hypothesis that leaves of local origin will harbor a more specialized community of aquatic bacteria, our results suggest that decomposition in streams of nonlocal leaves

requires a more diverse freshwater bacterial community than local leaves. We found that across different stages of succession, Away leaves tended to be inhabited by more diverse communities than Home leaves. Our metabolic functional predictions further suggest that these Away communities include many specialist taxa with the capacity to degrade aromatic compounds.

We focused our study on bacterial degradation of aromatic compounds because we had previously documented intraspecific variation in *A. rubra* leaves in several classes of aromatic secondary metabolites (i.e., ellagitannins and diarylheptanoids [see Fig. S2 and reference 10]). However, in addition to these aromatic defensive compounds, lignin is a ubiquitous aromatic polymer that lends structure to plant cell walls. Degradation of plant litter at both early and late stages of decomposition is regulated in part by lignin (33), and while studies of lignin decomposition have focused mostly on degradation pathways in fungi, more recent studies have reported that lignin degradation pathways also exist in some bacterial taxa (34). Further studies are necessary to disentangle the relative importance of lignin versus other classes of aromatic secondary metabolites in regulating bacterial community composition, bacterial metabolism, and rates of litter decomposition. However, knowing the precise makeup of aromatic compounds in each individual tree at the time of the experiment is not necessary to conclude that divergence in taxa capable of degrading aromatic compounds between Home and Away leaves is involved in locally accelerating decomposition.

We also found evidence in support of our second hypothesis, that the aquatic bacterial community inhabiting local leaves will undergo more rapid successional change than communities inhabiting leaves of nonlocal origin. Specifically, we found that Away communities appear to have a greater capacity for aromatic degradation at day 5, possibly indicating that Away leaves require a greater relative abundance and/or longer residence time of taxa capable of metabolizing locally novel plant secondary metabolites. Future studies that are more temporally resolved during this day 0 to 5 period would help clarify whether Away leaves have a greater abundance and longer residence time of taxa capable of degrading aromatics or whether Home leaves might have had equivalent or even greater capacity for aromatic degradation than Away leaves at some time prior to day 5. As these bacteria degrade plant secondary metabolites, later stages of succession may then sustain other bacterial taxa that can thrive on the subunits of the original plant metabolites, such as the successional patterns observed from primary to secondary consumers on marine particles (25). During later stages of decomposition, we found that freshwater bacterial communities no longer consisted largely of specialized taxa capable of degrading plant secondary metabolites but instead were dominated by generalists with enzymes capable of degrading cellulose, cellobiose, and simple carbohydrates.

The freshwater bacterial communities inhabiting leaves during the early stages of decomposition were dominated by two taxa of bacteria that are especially known for their capacity to degrade aromatics, the *Burkholderiales* and *Sphingomonadaceae* (35). Taxa within multiple families of *Burkholderiales* harbor genes that are key for the degradation of aromatics (36). Bacteria in the genus *Burkholderia* are especially important degraders of aromatic pollutants, and single strains can have multiple pathways for their degradation (37–39). The most abundant *Burkholderiales* taxa in our communities belonged to the *Comamonadaceae*, particularly *Comamonas* spp. Genome surveys of taxa within *Comamonadaceae* found that half of the taxa harbor dioxygenase genes required for the degradation of protocatechuate (36). Our results suggest that metagenome-level investigations of the *Burkholderiales* taxa in our study system may be warranted to help elucidate the role of these metabolic functions in locally accelerated decomposition. One could investigate whether the genetic architecture of these bacterial taxa explains their capacity of accelerated decomposition of local leaves, such as higher inherent rates of mutation or more rapid generation time. Further, plant polyphenols, such as the ellagitannins and diarylheptanoids common in red alder, are structurally analogous to anthropogenic, persistent polycyclic aromatics (6). Bioremediation strategies often take advantage of this structural similarity by using plant

secondary metabolites to boost the activity of microbes that can cometabolize both anthropogenic and natural aromatic hydrocarbons (6). Bacterial taxa that are fine tuned to spatial variation in plant secondary metabolites could perhaps be applied toward experimental evolution of improved degradation of anthropogenic aromatic pollutants (40).

We found that the bacterial communities of the terrestrial leaf phyllosphere partly contributed to the community that inhabited aquatic leaf packs using SourceTracker predictive models. We found that these taxa comprised an increasingly large portion of the leaf community later in succession, suggesting that populations of these taxa originating from the terrestrial environment tended to grow more than populations of taxa originating from the other source environments. Further study into how the phyllosphere would drive locally accelerated decomposition may be warranted. The living phyllosphere should travel within the leaf to the location of decomposition, where facilitative and/or antagonistic interactions with resident aquatic bacteria may then affect rates of decomposition. While it is challenging to explain how the home-field advantage might arise when most of the bacterial decomposer community originates from the phyllosphere, several fungus-based studies reach similar conclusions that fungal decomposers in soils are largely derived from the fungal community residing within the living phyllosphere (12, 41, 42). Unknown sources also contributed to the bacterial community inhabiting aquatic leaf packs. Unknown sources could include an environment that was not sampled, such as stream sediments. Alternatively, rare taxa residing in the sampled environments but below the level of detection might contribute to this unknown fraction. This might be especially common in our experiment because we surveyed varied habitats that would select for different bacterial physiologies. For example, a rare bacterium inhabiting the water column at a relative abundance below the level of detection may grow rapidly in population size once settling on a submerged leaf. Including quite different habitat types as potential sources may therefore limit predictions.

There are several limitations to our study. First, bacterial 16S rRNA surveys yield community composition data in terms of relative, not absolute, abundance. The limitations of relative abundance data are well appreciated, but acquiring absolute abundance measures remains challenging, particularly for bacterial communities inhabiting more complex environments. Quantities of extracted DNA are not suitable proxies for bacterial abundance due to many factors that influence extraction efficiency, such as leaf inhibitory compounds within leaf tissue. Newer methods for quantifying absolute abundance are actively being developed to overcome this limitation (43, 44). Second, an in-depth survey of temporal changes within bacterial communities came at the expense of broader spatial scope. We chose four sites within two study rivers close to each other because this proximity is what makes the observed patterns of locally accelerated decomposition particularly notable. While we have found similar patterns of locally accelerated decomposition in a second pair of rivers, without matching data in other systems, we caution that further studies are needed before generalizing these results more broadly to other river systems. Third, while our aim was to probe for the role of bacteria in degrading leaf secondary metabolites, other aromatic compounds are undoubtedly produced by decomposers. To infer a direct link of specific microbes to degrading plant secondary compounds, additional types of data are needed such as experiments using isotopically labeled plant secondary metabolites and metagenome surveys of bacteria and fungi. Further, it is important to note that our study used fresh green leaves rather than senescent leaf litter. These two types of leaf litter play key but different roles in stream nutrient cycles and food webs. Although some forested streams may receive minimal greenfall (less than 2.5% of total leaf fall [45]), some temperate rainforest streams can receive as much as ~20% of their annual leaf flux as greenfall (46). Although a smaller proportion of annual leaf fall, green leaf litter has greater nutrient content, including nitrogen, phosphorus, and potassium (45, 47), as well as a lower lignin-to-nitrogen ratio (48). This more nutrient-dense food source, which enters streams during the summer growing season for many aquatic organisms,

can have critical implications for stream productivity. For example, despite the greater abundance of autumnal leaf litter, phosphorus inputs from leaf litter per square meter of stream have been reported as 4 times higher in summer due to this higher nutrient content of green leaves (47). Further, when these fresh, nutrient-dense leaves are available, aquatic macroinvertebrates grow more rapidly than when only senescent leaves are available (49, 50). Further investigation into how nutrient cycles differ between streams receiving different proportions of leaf fluxes as greenfall is warranted. Although we do not have data on the secondary chemistry or decomposition patterns of senescent red alder leaves, given known differences between green and senescent litter reported elsewhere (51), testing whether our findings using green leaves apply when using senescent leaf litter would be a valuable future direction.

We also note that these results should also be considered in light of limitations inherent in using the PICRUSt tool. Metagenome predictions rely on the accuracy of 16S rRNA sequencing data to depict a microbial community. Primer biases can lead to inaccurate descriptions of bacterial communities, as well as omit the viral and eukaryotic components of microbial communities. Further, PICRUSt predictions are limited by the depth and accuracy of available databases. Genes lacking sufficient annotation may play critical functional roles but would go undetected with this approach. Further, a limitation of PICRUSt, particularly when using environmental samples, is that the tool predicts gene content using reference genomes. Therefore, accurate predictions depend on the availability of appropriate references (note: we have shown that our environmental samples have appropriate references by finding an average nearest sequences taxon index of $<0.10$). Despite these limitations, our results begin to shed light on the complex bacterial component of leaf decomposition in rivers.

Ninety percent of terrestrial plant biomass enters the detrital food webs of soils and freshwater ecosystems (52). Understanding biotic controls on rates of leaf decomposition is important as these rates affect the proportion of organic carbon that is locally metabolized and respired as $CO_2$, sequestered in the streambed, or exported further downstream. When paired with prior knowledge in this study system, the present study highlights how synchrony between leaf chemistry and local bacterial decomposers arises at small spatial scales and that disturbance of this synchronization significantly affects microbial community composition and function and, as a consequence, rates of decomposition. How these findings translate to predictions of long-term disturbance effects on carbon dynamics in riparian systems requires a better understanding of the underlying processes governing microbial community assembly, selection, and dispersal.

A key challenge is identifying mechanisms that may promote resilience of ecosystem function in the face of environmental change. Microbial components may offer important contributions to ecosystem resilience through their wide-ranging biochemical pathways and their high physiological, generational, and evolutionary rates. Our findings documenting changes through time and fine-scale environmental matching lend strong support to the notion that microbial community components can play a central role in stabilizing ecosystem function in a changing environment.

## MATERIALS AND METHODS

**Study site.** We studied decomposition of leaf litter in two rivers of the Olympic Peninsula of Washington State, USA. The Sekiu and Hoko Rivers are fourth-order streams with riparian forest comprised mostly of red alder (*Alnus rubra*), small numbers of bigleaf maple (*Acer macrophyllum*), and few conifers. We identified two reaches per stream that we refer to as upstream and downstream because their orientation relative to one another is important for the study design; however, all of the study reaches are relatively far downstream near the river mouths. Additional details regarding location, river morphology, and environmental characteristics can be found in reference 11.

**Field experiment.** We previously found that red alder trees vary geographically in leaf traits that strongly influence the rate of leaf decomposition in riparian soils and rivers (10). Here, we repeated our test of the effects of individual variation on leaf litter decomposition in streams, while simultaneously testing the effects of this variation on the composition of the bacterial decomposer community and the metabolic pathways associated with that community. We conducted a reciprocal transplant experiment of red alder leaf packs across two rivers in August 2013. The Hoko and Sekiu Rivers are approximately 4.5 km apart. Our upstream and downstream sites within each river were less than 1 km apart. We

identified 10 trees in the riparian zones of the Sekiu River and 10 trees in the riparian zone of the Hoko River. Within each river, five riparian red alder trees were growing immediately upstream of the "upstream" incubation site, and five trees were growing immediately upstream of the "downstream" incubation site. Our incubation sites were at the most downstream section of each study reach, so that leaves from all riparian trees identified at that study reach would float downriver toward the incubation site (see Fig. S1 in the supplemental material for an illustration of the study design). Within each study reach, we deployed leaf packs onto the streambed using steel reinforcement bars.

For our experiment, we used only fresh green leaves to construct our leaf packs. Compared to brown, senescent leaves, green leaves decompose rapidly in streams, support high aquatic invertebrate diversity, and fall into rivers in large quantities during the summer growing season (49). We found that over 60% of red alder leaf litter is still green upon entering rivers of the Olympic Peninsula of Washington in summer (11). In the Hoko River, this equated to 96 $g \cdot m^{-1} \cdot day^{-1}$ of green leaf material from red alder trees entering the river in July and August of 2012. We chose to use green leaves because our finding that intraspecific variation in *A. rubra* secondary chemistry causes local leaves to decompose more rapidly was done using green leaves. Whether a home-field advantage pattern occurs using senescent leaves of *A. rubra* has not yet been tested. We manually detached green leaves for use in our experiments rather than collect greenfall to enable collection of a large number of leaves that had been detached from their parent tree for a standardized amount of time, as well as to control for tree of origin.

From each red alder tree, we constructed four replicates of leaf packs that we deployed at each of the four incubation sites, including the "Home Site" that was immediately downstream of the source tree, the "Away Site" on the same river where the source tree was growing, and the "Away River, Upstream" and "Away River, Downstream" sites on the paired study river. Each of these leaf packs contained 16 leaves from a single alder tree. Twelve of these leaves were preweighed and dedicated to determining percent leaf mass loss. A mesh bag of these 12 leaves was placed into a second outer mesh bag that contained the remaining four leaves used for bacterial sequencing. We used only leaves with minimal visible damage from herbivores and disease. We collected one leaf from each of the outer mesh bags of each leaf pack after 5, 10, 15, and 20 days of incubation and sealed each leaf individually in a sterile Whirl-Pak bag. The remaining 12 leaves from each inner mesh bag of each leaf pack were blotted dry with paper towels and weighed to measure percent leaf mass remaining after 21 days of incubation. Although these inner leaf packs lost at most only a third of initial leaf mass over the 21-day incubation (maximum lost = 29.6%, mean lost = 10.6% ± 0.8% [SE]), it is important to note that this is not representative of the amount of leaf mass lost by leaves collected on day 20 for bacterial surveys. Leaves collected for bacterial surveys were from the outer mesh bags of the leaf pack, which decomposed considerably more than inner leaves. By 20 days, leaves in the outer leaf pack that were used for 16S rRNA sequencing were in the later stages of decomposition as indicated by a thin, skeletonized leaf completely black in color with little remaining structure. Based on our prior leaf pack studies in this system, we estimate our day 20 leaves would have disintegrated entirely within 1 to 5 extra days of incubation.

We sampled the freshwater bacterial community at each incubation site immediately prior to deploying our leaf pack experiment, as well as prior to leaf collections on days 5, 10, 15, and 20. Each sample consisted of up to 6 liters of river water pumped through a Sterivex filter (EMD Millipore, Darmstadt, Germany) with a peristaltic pump. Immediately before the 20-day experiment, we collected riparian soil samples beneath each source tree and green fresh leaves from each tree. All samples were frozen at −20°C immediately upon returning from the field locations and then stored at −80°C until processing.

**Bacterial sequencing.** We extracted DNA from all soil, water, and leaf samples using PowerSoil DNA isolation kits (Mo Bio Laboratories, Carlsbad, CA, USA). We used the identical extraction protocol for all samples to facilitate comparisons within our data set, as well as to meet the goals of the broader Earth Microbiome Project research collaborative to use standardized methods to best facilitate data syntheses. For water samples, Sterivex casings were cut with polyvinyl chloride (PVC) cutters and half of the filter paper was removed and then ground and extracted as a solid sample. We amplified the 254-bp length V4 region of extracted DNA using the Earth Microbiome Project universal primers (515F primer and 806 GoLay-barcoded reverse primers) (53). We chose not to use mitochondrial and chloroplast blocking peptide nucleic acid (PNA) clamps during PCR amplification due to our prior finding that use of the chloroplast pPNA sequence biases amplification of certain bacterial taxa (54, 55). We sequenced DNA fragments in a HiSeq 2500 2- by 151-bp run at the Environmental Sample Preparation and Sequencing facility at Argonne National Laboratory according to the procedures of Caporaso et al. (53). In brief, all bacterial sequencing data were analyzed using the QIIME pipeline. We assigned taxonomy to all 16S rRNA sequences using the Greengenes database, which was preferable for our study because of its compatibility with the functional annotation tool PICRUSt (Phylogenetic Investigation of Communities by Reconstruction of Unobserved States) (22). We used this PICRUSt software package to predict metagenome functional content by using ancestral-state reconstruction as a means of predicting the presence of gene families. We then used the Kyoto Encyclopedia of Genes and Genomes (KEGG) database to identify genes within certain functional pathways that we had hypothesized might play key roles in leaf degradation (i.e., pathways for the degradation of aromatic compounds, starch, sucrose, and cellulose). To predict where bacterial communities that inhabited our leaf packs originated, we used Bayesian SourceTracker models with a uniform prior for each of our known source environments (i.e., riparian soil, terrestrial leaves, and the water column) (20). For details of all data analyses, see Text S1 in the supplemental material.

**Data accessibility.** All sequencing data have been permanently deposited at https://www.ncbi.nlm.nih.gov/Traces/study/?acc=PRJNA525284 (accession no. PRJNA525284).

## SUPPLEMENTAL MATERIAL

Supplemental material for this article may be found at https://doi.org/10.1128/mBio.01703-19.

**TEXT S1**, PDF file, 0.2 MB.
**FIG S1**, PDF file, 0.2 MB.
**FIG S2**, PDF file, 0.3 MB.
**FIG S3**, PDF file, 0.5 MB.
**FIG S4**, PDF file, 0.1 MB.
**FIG S5**, PDF file, 0.8 MB.
**FIG S6**, PDF file, 0.3 MB.
**FIG S7**, PDF file, 0.6 MB.
**FIG S8**, PDF file, 0.2 MB.
**TABLE S1**, PDF file, 0.1 MB.

## ACKNOWLEDGMENTS

We thank C. Pfister, V. Denef, T. Price, J. Bergelson, and G. Dwyer for constructive comments and discussion on this work. We also thank S. Owens, S. Greenwald, N. Sangwan, S. Gibbons, J. Hampton-Marcell, A. Frazier, N. Gottel, S. Lax, R. Props, and M. Schmidt for assistance and advice with sequencing and analyses. We thank J. Murray, M. Hurd, D. Hurd, Hoko River State Park, and the Washington State Department of Natural Resources for providing facilities and facilitating research on their lands.

This work was supported by NSF DEB-1556874 to J.T.W., and the NSF GRFP, the DOE GAANN, NSF DDIG DEB-1311293, the ARCS (Achievement Rewards for College Scientists) Foundation, Inc.'s Scholar Illinois Chapter (2014 and 2015), a National Geographic Young Explorer's Grant, and the American Society of Naturalists' Student Research Award to S.L.J.

## REFERENCES

1. Ehrlich PR, Raven PH. 1964. Butterflies and plants: a study in coevolution. Evolution 18:586–608. https://doi.org/10.2307/2406212.
2. Farrell BD, Dussourd DE, Mitter C. 1991. Escalation of plant defense: do latex and resin canals spur plant diversification? Am Nat 138:881–900. https://doi.org/10.1086/285258.
3. Hartmann T. 2007. From waste products to ecochemicals: fifty years research of plant secondary metabolism. Phytochemistry 68:2831–2846. https://doi.org/10.1016/j.phytochem.2007.09.017.
4. Mithöfer A, Boland W. 2012. Plant defense against herbivores: chemical aspects. Annu Rev Plant Biol 63:431–450. https://doi.org/10.1146/annurev-arplant-042110-103854.
5. Rosenthal GA, Berenbaum MR. 2012. Herbivores: their interactions with secondary plant metabolites: ecological and evolutionary processes, vol 2. Academic Press, New York, NY.
6. Singer AC, Crowley DE, Thompson IP. 2003. Secondary plant metabolites in phytoremediation and biotransformation. Trends Biotechnol 21:123–130. https://doi.org/10.1016/S0167-7799(02)00041-0.
7. Hall RO, Jr, Meyer JL. 1998. The trophic significance of bacteria in a detritus-based stream food web. Ecology 79:1995–2012. https://doi.org/10.2307/176704.
8. Rudman SM, Kreitzman M, Chan KM, Schluter D. 2017. Evosystem services: rapid evolution and the provision of ecosystem services. Trends Ecol Evol 32:403–415. https://doi.org/10.1016/j.tree.2017.02.019.
9. Gholz HL, Wedin DA, Smitherman SM, Harmon ME, Parton WJ. 2000. Long-term dynamics of pine and hardwood litter in contrasting environments: toward a global model of decomposition. Glob Chang Biol 6:751–765. https://doi.org/10.1046/j.1365-2486.2000.00349.x.
10. Jackrel SL, Morton TC, Wootton JT. 2016. Intraspecific leaf chemistry drives locally accelerated ecosystem function in aquatic and terrestrial communities. Ecology 97:2125–2135. https://doi.org/10.1890/15-1763.1.
11. Jackrel SL, Wootton JT. 2014. Local adaptation of stream communities to intraspecific variation in a terrestrial ecosystem subsidy. Ecology 95:37–43. https://doi.org/10.1890/13-0804.1.
12. Austin AT, Vivanco L, González-Arzac A, Pérez LI. 2014. There's no place like home? An exploration of the mechanisms behind plant litter–decomposer affinity in terrestrial ecosystems. New Phytol 204:307–314. https://doi.org/10.1111/nph.12959.
13. Ayres E, Steltzer H, Simmons BL, Simpson RT, Steinweg JM, Wallenstein MD, Mellor N, Parton WJ, Moore JC, Wall DH. 2009. Home-field advantage accelerates leaf litter decomposition in forests. Soil Biol Biochem 41:606–610. https://doi.org/10.1016/j.soilbio.2008.12.022.
14. Jackrel SL, Wootton JT. 2015. Diversity of riparian plants among and within species shapes river communities. PLoS One 10:e0142362. https://doi.org/10.1371/journal.pone.0142362.
15. Kominoski JS, Marczak LB, Richardson JS. 2011. Riparian forest composition affects stream litter decomposition despite similar microbial and invertebrate communities. Ecology 92:151–159. https://doi.org/10.1890/10-0028.1.
16. Hieber M, Gessner MO. 2002. Contribution of stream detrivores, fungi, and bacteria to leaf breakdown based on biomass estimates. Ecology 83:1026–1038. https://doi.org/10.1890/0012-9658(2002)083[1026:COSDFA]2.0.CO;2.
17. Tank JL, Rosi-Marshall EJ, Griffiths NA, Entrekin SA, Stephen ML. 2010. A review of allochthonous organic matter dynamics and metabolism in streams. J N Am Benthol Soc 29:118–146. https://doi.org/10.1899/08-170.1.
18. Wallace JB, Webster JR. 1996. The role of macroinvertebrates in stream ecosystem function. Annu Rev Entomol 41:115–139. https://doi.org/10.1146/annurev.en.41.010196.000555.
19. Lozupone C, Knight R. 2005. UniFrac: a new phylogenetic method for comparing microbial communities. Appl Environ Microbiol 71:8228–8235. https://doi.org/10.1128/AEM.71.12.8228-8235.2005.
20. Knights D, Kuczynski J, Charlson ES, Zaneveld J, Mozer MC, Collman RG, Bushman FD, Knight R, Kelley ST. 2011. Bayesian community-wide culture-independent microbial source tracking. Nat Methods 8:761. https://doi.org/10.1038/nmeth.1650.
21. Jousset A, Bienhold C, Chatzinotas A, Gallien L, Gobet A, Kurm V, Küsel K, Rillig MC, Rivett DW, Salles JF, van der Heijden MGA, Youssef NH, Zhang X, Wei Z, Hol WHG. 2017. Where less may be more: how the rare biosphere pulls ecosystems strings. ISME J 11:853. https://doi.org/10.1038/ismej.2016.174.

22. Langille MGI, Zaneveld J, Caporaso JG, McDonald D, Knights D, Reyes JA, Clemente JC, Burkepile DE, Vega Thurber RL, Knight R, Beiko RG, Huttenhower C. 2013. Predictive functional profiling of microbial communities using 16S rRNA marker gene sequences. Nat Biotechnol 31:814. https://doi.org/10.1038/nbt.2676.
23. Duffy JE, Godwin CM, Cardinale BJ. 2017. Biodiversity effects in the wild are common and as strong as key drivers of productivity. Nature 549:261. https://doi.org/10.1038/nature23886.
24. Faith DP. 1992. Conservation evaluation and phylogenetic diversity. Biol Conserv 61:1–10. https://doi.org/10.1016/0006-3207(92)91201-3.
25. Datta MS, Sliwerska E, Gore J, Polz MF, Cordero OX. 2016. Microbial interactions lead to rapid micro-scale successions on model marine particles. Nat Commun 7:11965. https://doi.org/10.1038/ncomms11965.
26. Metcalf JL, Xu ZZ, Weiss S, Lax S, Van Treuren W, Hyde ER, Song SJ, Amir A, Larsen P, Sangwan N, Haarmann D, Humphrey GC, Ackermann G, Thompson LR, Lauber C, Bibat A, Nicholas C, Gebert MJ, Petrosino JF, Reed SC, Gilbert JA, Lynne AM, Bucheli SR, Carter DO, Knight R. 2016. Microbial community assembly and metabolic function during mammalian corpse decomposition. Science 351:158–162. https://doi.org/10.1126/science.aad2646.
27. Teeling H, Fuchs BM, Becher D, Klockow C, Gardebrecht A, Bennke CM, Kassabgy M, Huang S, Mann AJ, Waldmann J, Weber M, Klindworth A, Otto A, Lange J, Bernhardt J, Reinsch C, Hecker M, Peplies J, Bockelmann FD, Callies U, Gerdts G, Wichels A, Wiltshire KH, Glöckner FO, Schweder T, Amann R. 2012. Substrate-controlled succession of marine bacterioplankton populations induced by a phytoplankton bloom. Science 336:608–611. https://doi.org/10.1126/science.1218344.
28. Tláskal V, Zrůstová P, Vrška T, Baldrian P 2017. Bacteria associated with decomposing dead wood in a natural temperate forest. FEMS Microbiol Ecol 93:fix157. https://doi.org/10.1093/femsec/fix157.
29. Marks JC, Haden G, Harrop BL, Reese EG, Keams JL, Watwood ME, Whitham TG. 2009. Genetic and environmental controls of microbial communities on leaf litter in streams. Freshw Biol 54:2616–2627. https://doi.org/10.1111/j.1365-2427.2009.02270.x.
30. Biere A, Marak HB, van Damme JM. 2004. Plant chemical defense against herbivores and pathogens: generalized defense or trade-offs? Oecologia 140:430–441. https://doi.org/10.1007/s00442-004-1603-6.
31. Dodds PN, Rathjen JP. 2010. Plant immunity: towards an integrated view of plant-pathogen interactions. Nat Rev Genet 11:539. https://doi.org/10.1038/nrg2812.
32. Fanin N, Fromin N, Bertrand I. 2016. Functional breadth and home-field advantage generate functional differences among soil microbial decomposers. Ecology 97:1023–1037.
33. Klotzbücher T, Kaiser K, Guggenberger G, Gatzek C, Kalbitz K. 2011. A new conceptual model for the fate of lignin in decomposing plant litter. Ecology 92:1052–1062. https://doi.org/10.1890/10-1307.1.
34. Bugg TD, Ahmad M, Hardiman EM, Rahmanpour R. 2011. Pathways for degradation of lignin in bacteria and fungi. Nat Prod Rep 28:1883–1896. https://doi.org/10.1039/c1np00042j.
35. Ghosal D, Ghosh S, Dutta TK, Ahn Y. 2016. Current state of knowledge in microbial degradation of polycyclic aromatic hydrocarbons (PAHs): a review. Front Microbiol 7:1369. https://doi.org/10.3389/fmicb.2016.01837.
36. Pérez-Pantoja D, Donoso R, Agulló L, Córdova M, Seeger M, Pieper DH, González B. 2012. Genomic analysis of the potential for aromatic compounds biodegradation in Burkholderiales. Environ Microbiol 14:1091–1117. https://doi.org/10.1111/j.1462-2920.2011.02613.x.
37. Chain PSG, Denef VJ, Konstantinidis KT, Vergez LM, Agullo L, Reyes VL, Hauser L, Cordova M, Gomez L, Gonzalez M, Land M, Lao V, Larimer F, LiPuma JJ, Mahenthiralingam E, Malfatti SA, Marx CJ, Parnell JJ, Ramette A, Richardson P, Seeger M, Smith D, Spilker T, Sul WJ, Tsoi TV, Ulrich LE, Zhulin IB, Tiedje JM. 2006. Burkholderia xenovorans LB400 harbors a multi-replicon, 9.73-Mbp genome shaped for versatility. Proc Natl Acad Sci U S A 103:15280–15287. https://doi.org/10.1073/pnas.0606924103.
38. Denef V, Klappenbach J, Patrauchan M, Florizone C, Rodrigues J, Tsoi T, Verstraete W, Eltis L, Tiedje J. 2006. Genetic and genomic insights into the role of benzoate-catabolic pathway redundancy in Burkholderia xenovorans LB400. Appl Environ Microbiol 72:585–595. https://doi.org/10.1128/AEM.72.1.585-595.2006.
39. Denef V, Park J, Tsoi T, Rouillard J-M, Zhang H, Wibbenmeyer J, Verstraete W, Gulari E, Hashsham S, Tiedje J. 2004. Biphenyl and benzoate metabolism in a genomic context: outlining genome-wide metabolic networks in Burkholderia xenovorans LB400. Appl Environ Microbiol 70:4961–4970. https://doi.org/10.1128/AEM.70.8.4961-4970.2004.
40. Gilbert ES, Crowley DE. 1997. Plant compounds that induce polychlorinated biphenyl biodegradation by Arthrobacter sp. strain B1B. Appl Environ Microbiol 63:1933–1938.
41. Peršoh D. 2013. Factors shaping community structure of endophytic fungi—evidence from the Pinus-Viscum-system. Fungal Divers 60:55–69. https://doi.org/10.1007/s13225-013-0225-x.
42. Voříšková J, Baldrian P 2013. Fungal community on decomposing leaf litter undergoes rapid successional changes. ISME J 7:477. https://doi.org/10.1038/ismej.2012.116.
43. Props R, Kerckhof F-M, Rubbens P, De Vrieze J, Sanabria EH, Waegeman W, Monsieurs P, Hammes F, Boon N. 2017. Absolute quantification of microbial taxon abundances. ISME J 11:584. https://doi.org/10.1038/ismej.2016.117.
44. Smets W, Leff JW, Bradford MA, McCulley RL, Lebeer S, Fierer N. 2016. A method for simultaneous measurement of soil bacterial abundances and community composition via 16S rRNA gene sequencing. Soil Biol Biochem 96:145–151. https://doi.org/10.1016/j.soilbio.2016.02.003.
45. Risley LS, Crossley D, Jr. 1988. Herbivore-caused greenfall in the southern Appalachians. Ecology 69:1118–1127. https://doi.org/10.2307/1941266.
46. Campbell I, Fuchshuber L. 1994. Amount, composition and seasonality of terrestrial litter accession to an Australian cool temperate rainforest stream. Arch Hydrobiol 130:499–512.
47. McArthur JV, Leff LG, Kovacic DA, Jaroscak J. 1986. Green leaf decomposition in Coastal Plain streams. J Freshw Ecol 3:553–558. https://doi.org/10.1080/02705060.1986.9665149.
48. Fonte SJ, Schowalter TD. 2004. Decomposition of greenfall vs. senescent foliage in a tropical forest ecosystem in Puerto Rico. Biotropica 36:474–482. https://doi.org/10.1646/1597.
49. Stout RJ, Taft WH, Merritt RW. 1985. Patterns of macroinvertebrate colonization on fresh and senescent alder leaves in two Michigan streams. Freshw Biol 15:573–580. https://doi.org/10.1111/j.1365-2427.1985.tb00227.x.
50. Kochi K, Kagaya T. 2005. Green leaves enhance the growth and development of a stream macroinvertebrate shredder when senescent leaves are available. Freshw Biol 50:656–667. https://doi.org/10.1111/j.1365-2427.2005.01353.x.
51. Hättenschwiler S, Vitousek PM. 2000. The role of polyphenols in terrestrial ecosystem nutrient cycling. Trends Ecol Evol 15:238–243. https://doi.org/10.1016/S0169-5347(00)01861-9.
52. Gessner MO, Swan CM, Dang CK, McKie BG, Bardgett RD, Wall DH, Hättenschwiler S. 2010. Diversity meets decomposition. Trends Ecol Evol 25:372–380. https://doi.org/10.1016/j.tree.2010.01.010.
53. Caporaso JG, Lauber CL, Walters WA, Berg-Lyons D, Huntley J, Fierer N, Owens SM, Betley J, Fraser L, Bauer M, Gormley N, Gilbert JA, Smith G, Knight R. 2012. Ultra-high-throughput microbial community analysis on the Illumina HiSeq and MiSeq platforms. ISME J 6:1621. https://doi.org/10.1038/ismej.2012.8.
54. Jackrel SL, Owens SM, Gilbert JA, Pfister CA. 2017. Identifying the plant-associated microbiome across aquatic and terrestrial environments: the effects of amplification method on taxa discovery. Mol Ecol Resour 17:931–942. https://doi.org/10.1111/1755-0998.12645.
55. Lundberg DS, Yourstone S, Mieczkowski P, Jones CD, Dangl JL. 2013. Practical innovations for high-throughput amplicon sequencing. Nat Methods 10:999. https://doi.org/10.1038/nmeth.2634.

## ELECTRONIC SUPPLEMENTARY MATERIALS

**Fig. S1.** Illustration of experimental design for the reciprocal transplant experiment. Also listed are measurements of temperature, photosynthetically active radiation (PAR), flow rate, conductivity, pH and dissolved oxygen from July 2013 for each of the four sites used in the reciprocal transplant experiment. Measures of temperature and PAR are means over 7 day periods, except for the Sekiu upstream site (2 days). Daytime temperatures were determined from 10 min interval readings using HOBO data loggers for all non-zero light measurements. Maximum and minimum temperatures include daytime and nighttime readings. Flow rates were measured during 0.5 min increments using a Global Water flow probe. Dissolved oxygen, conductivity, and pH were measured using a Hach HQ40d multiprobe.

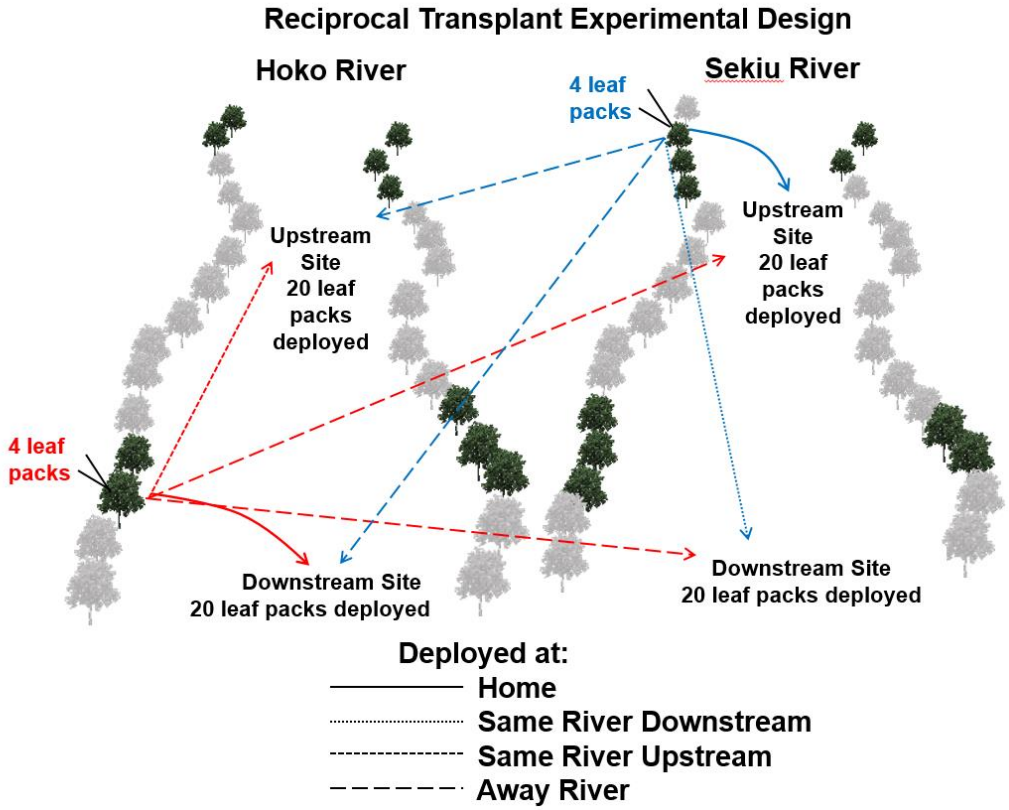


| River: | Sekiu | | Hoko | |
|---|---|---|---|---|
| Upstream; Downstream | Up | Down | Up | Down |
| Latitude (48°N+ °) | 0.165 | 0.165 | 0.153 | 0.154 |
| Longitude (124°W+ °) | 0.245 | 0.244 | 0.211 | 0.211 |
| Average temperature (°C) | 16.1 | 15.9 | 16.7 | 16.2 |
| Minimum temperature (°C) | 14.1 | 13.9 | 14.1 | 13.9 |
| Maximum temperature (°C) | 18.2 | 18.9 | 19.8 | 18.8 |
| PAR (µmol $m^{-2}s^{-1}$) | 5677 | 8478 | 8304 | 18567 |
| Width (m) | 24.6 | 16.5 | 12.8 | 23.3 |
| Depth (cm) | 46 | 35 | 36 | 30 |
| Flow rate (cm/s) | 1.75 | 1.43 | 4.14 | 1.86 |
| pH | 5.82 | 5.75 | 5.88 | 5.9 |
| Conductivity (µS/cm) | 74.2 | 72.7 | 80.5 | 75.3 |
| Dissolved oxygen (mg/L) | 8.48 | 8.91 | 9.61 | 9.39 |

## ELECTRONIC SUPPLEMENTARY MATERIALS

**Fig. S2.** (A) Leaves of individual red alder trees growing in the riparian zones of two rivers vary in the relative abundance of 35 secondary metabolites, including ellagitannins and diaryheptanoids, by tree origin via discriminant function analysis. (B) Loadings of each chemical variable, with tentative chemical ID, are shown in the corresponding table. (C) We also show compound characterizations for each of the 35 secondary metabolites. Where possible, we include tentative identifications of each compound, as well as retention time, diagnostic ions, exact mass, references, metabolomics confidence score, and mean fraction (± 1 SD) base peak chromatogram ion counts per milligram of red alder leaf tissue. Note that this table is reproduced from Jackrel et al. 2016. Also note that all leaf chemistry analyses were completed on leaves collected during the 2012 growing season. We also used leaves from these same trees in reciprocal transplant leaf pack experiments that were designed to test whether decomposer communities decompose local leaves more rapidly than non-local leaves (i.e. Home-Field Advantage). One experiment first reported in Jackrel and Wootton (2014) was completed in 2012 using leaves from the 2012 growing season. A second experiment was completed in 2013 using leaves from the 2013 growing season. Both experiments suggested a home-field advantage as calculated using the method reported by Ayres et al. 2009 (2013: $t_9 = 2.60$, $p = 0.014$, 2012: $t_9 = 1.96$, $p = 0.041$).

(A)

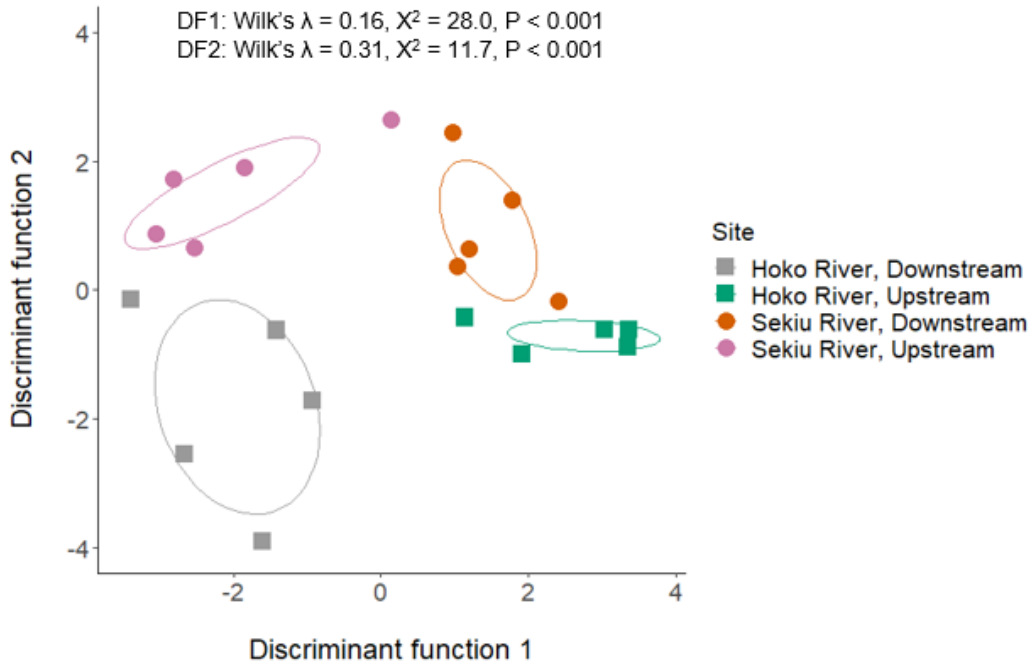

(B)

| Peak # | Chemical ID | DF1 | DF2 |
|---|---|---|---|
| 1 | | -0.39 | 0.10 |
| 2 | | -0.63 | 0.00 |
| 3 | HHDP-Glucose | 0.40 | -0.35 |
| 4 | HHDP-Glucose | -0.46 | 0.45 |
| 5 | galloyl glucose | -0.09 | 0.01 |
| 6 | di-HHDP-glucose (Pedunculagin B) | 0.10 | -0.20 |
| 7 | di-HHDP-glucose (Pedunculagin a) | -0.17 | 0.46 |
| 8 | HHDP-galloyl-glucose (Isostrictinin) | -0.34 | -0.16 |
| 9 | di-galloyl-HHDP-glucose (Tellimagrandin I B) | 0.16 | 0.48 |
| 10 | HHDP-galloyl-glucose (Strictinin) | -0.55 | 0.01 |
| 11 | | 0.10 | 0.09 |
| 12 | di-galloyl-HHDP-glucose (Tellimagrandin I a) | -0.02 | 0.32 |
| 13 | | 0.71 | 0.10 |
| 14 | | -0.42 | 0.10 |
| 15 | di-HHDP-galloyl-glucose B (Casuarictin) | 0.00 | 0.08 |
| 16 | di-HHDP-galloyl-glucose a | -0.61 | 0.05 |
| 17 | | 0.87 | -0.68 |
| 18 | tri-O-galloyl-HHDP-glucose | -0.19 | 0.23 |
| 19 | | -0.34 | 0.49 |
| 20 | | 0.76 | -0.58 |
| 21 | | 0.38 | -1.02 |
| 22 | tri-O-galloyl-HHDP-glucose | 0.05 | 0.36 |
| 23 | HOG | 0.74 | 0.02 |
| 24 | Oregonin | -0.41 | -0.01 |
| 25 | Quercitin-glucuronide | -0.40 | -0.01 |
| 26 | Alnuside A | 0.74 | 0.27 |
| 27 | Alnuside B | -0.28 | 0.98 |
| 28 | | 0.13 | 0.36 |
| 29 | Quercitin-rhamnoside | -0.03 | 0.07 |
| 30 | Methylhirsutanonol | 0.18 | -0.18 |
| 31 | platyphylanolanol-xyloside | 0.01 | 0.62 |
| 32 | Hirsutanone | 0.09 | -0.03 |
| 33 | | -0.50 | -0.10 |
| 34 | novel diarylheptanoid | -0.41 | 0.11 |
| 35 | Alnuside C | 0.22 | -0.24 |

(C)

| Peak | RT (secs) | TIC % Area | M-H (%) | Exact Mass | Diff (ppm) | Diagnostic ions/TIC% first | second | third | fourth | Refs | Annotation Level[6] | Chemical ID, formula (MH-) and (oxidation activity abs/s/mM) |
|---|---|---|---|---|---|---|---|---|---|---|---|---|
| 1 | 115 | 1.7 ± 1.2 | | | | 122.92/100 | 206.88/50 | | | | 4 | |
| 2 | 140 | 5.7 ± 2.6 | | | | 191.05/100 | 267.15/20 | 405.09 | | | 4 | |
| 3 | 200 | 2.0 ± 1.5 | 481.0612 (25) | 481.0624 | -1.18 | 300.9976/100 | | | | 1,2 | 3 | HHDP-Glucose, $C_{20}H_{17}O_{14}$ (3) |
| 4 | 270 | 1.2 ± 0.80 | 481.0632 (25) | 481.0624 | +0.82 | 300.9998/100 | | | | 1,2 | 3 | HHDP-Glucose, $C_{20}H_{17}O_{14}$ (3) |
| 5 | 510 | 0.28 ± 0.21 | 331.0636 (100) | 331.0612 | -3.47 | 169.0119/60 | | | | 1,2 | 3 | galloyl glucose, $C_{13}H_{15}O_{10}$ (0) |
| 6 | 1100 | 7.4 ± 3.3 | 783.0726 (80) | 783.0668 | +3.95 | 300.99/100 | 481.0658 | 301.0015 | 169.0147 | 1,2 | 3 | di-HHDP-glucose, (Pedunculagin β), $C_{34}H_{22}O_{22}$ (5) |
| 7 | 1190 | 9.8 ± 2.5 | 783.0699 (80) | 783.0668 | +1.25 | 300.99/100 | 481.0632 | 301 | 169.0147 | 1,2 | 3 | di-HHDP-glucose (Pedunculagin α), $C_{34}H_{22}O_{22}$ (5) |
| 8 | 1250 | 3.1 ± 0.61 | 633.0739 (25) | 633.0733 | +0.56 | 300.9908/100 | 275.01/20 | | | 1,2 | 3 | HHDP-galloyl-glucose (Isostrictinin), $C_{27}H_{21}O_{18}$ (4.9) |
| 9 | 1295 | 5.0 ± 0.73 | 785.0797 (80) | 785.0843 | -4.60 | 300.99/100 | 275.0213/25 | 829.07/10 | | 1,2 | 3 | di-galloyl-HHDP-glucose(Tellimagrandin Iβ),$C_{34}H_{25}O_{22}$ (3.3) |
| 10 | 1370 | 4.8 ± 1.4 | 633.0726 (25) | 633.0733 | -0.74 | 300.9908/100 | 275.01/20 | | | 1,2 | 3 | HHDP-galloyl-glucose (Strictinin), $C_{27}H_{21}O_{18}$ (3) |
| 11 | 1401 | 1.4 ± 0.51 | 965.0825 (4) | | | 124.0154/100 | 183.029/15 | 300.9998/13 | 783.0692 | | 4 | too small, but major galloyl in + |
| 12 | 1427 | 3.7 ± 1.2 | 785.0882 (86) | 785.0855 | +3.90 | 300.9978/100 | 483.0692/2 | 481.0516/0.3 | 169.01285/12 | 1,2 | 3 | di-galloyl-HHDP-glucose(Tellimagrandin Iα),$C_{34}H_{23}O_{22}$ (3.3) |
| 13 | 1445 | 1.5 ± 0.31 | 965.0748 (2) | | | 300.99/100 | 169.0136/35 | 483.0728/27 | 635.0744/3 | | 4 | |
| 14 | 1467 | 2.0 ± 2.2 | | | | 191.0529/100 | 375.0607/14 | 633.0561/1 | 729.1375/1 | | 4 | derivative of chlorogenic acid |
| 15 | 1491 | 4.9 ± 0.94 | 935.0857 (57) | 935.0737 | -1.8 | 300.99/100 | 785.0676/2 | 633.0622/14 | 169.01/3 | 1,2 | 3 | di-HHDP-galloyl-glucose β (Casuarictin), $C_{41}H_{27}O_{26}$ (4.1) |
| 16 | 1525 | 1.7 ± 0.43 | 935.0789 (21) | 935.0737 | 0.7 | 300.99/100 | 785.0723/2 | 633.0656/10 | 169.0128/4 | 1,2 | 3 | di-HHDP-galloyl-glucose α, $C_{41}H_{27}O_{26}$ (4.1) |
| 17 | 1550 | 1.3 ± 0.24 | | | | 300.99/100 | 169.013/55 | 635.0781/8 | 465.0605/12 | | 4 | |
| 18 | 1570 | 3.1 ± 1.3 | 937.0929 (39) | 937.0952 | -2.35 | 300.99/100 | 767.0562/2 | 465.0658/9 | 169.0141/20 | 1,2 | 3 | tri-O-galloyl-HHDP-glucose (β?), $C_{41}H_{29}O_{26}$ (2) |
| 19 | 1610 | 3.0 ± 1.0 | 1025.07 (2) | | | 300.99/100 | 191/15 | 169/6 | | | 4 | derivative of chlorogenic acid |
| 20 | 1675 | 1.3 ± 0.52 | | | | 300.99/100 | | | | | 4 | |
| 21 | 1705 | 1.7 ± 0.28 | 997.08 (4) | | | 300.99/100 | 617.06/4 | 757.077/8 | 169.01/10 | | 4 | |
| 22 | 1740 | 1.7 ± 0.64 | 937.0961 (17) | 937.0952 | +0.85 | 300.99/100 | 785.0707/2 | 465.0562/3 | 169.0152/12 | 1,2 | 3 | tri-O-galloyl-HHDP-glucose (α?), $C_{41}H_{29}O_{26}$ (2) |
| 23 | 1780 | 1.1 ± 0.89 | 507.1871 (17) | 507.1872 | -0.09 | 205.0874/100 | 327.1249/34 | 121.02/90 | | 3 | 2 | HOG*, $C_{25}H_{31}O_{11}$ |
| 24 | 1840 | 7.8 ± 3.4 | 477.1751 (45) | 477.1766 | -1.52 | 205.0874/60 | 121.02/100 | 327.1249/53 | | 3 | 1 | Oregonin**, $C_{24}H_{29}O_{10}$ |
| 24a | 1915 | | 491.1925 (4) | 491.1922 | +0.23 | 121.0284/100 | 311.12/41 | 205.083/56 | 189.087/38 | 3,4 | 2 | Related to Alnuside B with glucose, $C_{25}H_{30}O_{10}$ |
| 25 | 1960 | 7.6 ± 2.5 | 477.0666 (55) | 477.0675 | -0.86 | 301.0273/100 | 150.9997/24 | 255.0212/4 | 178.9932/8 | 5 | 2 | Quercitin-glucuronide, $C_{21}H_{17}O_{13}$ |
| 25a | 1971 | | 463.0899 (100) | 463.0882 | +1.70 | 271.0226/89 | 300.024/88 | 301.029/51 | 255.0267/35 | 5 | 2 | Quercitin-glucoside, $C_{21}H_{19}O_{12}$ |
| 26 | 2025 | 0.25 ± 0.29 | 461.1858(2) | 461.1817 | +4.19 | 311.1322 | 121.0308/62 | 205.0901/18 | 189.0943/6 | 3 | 2 | Alnuside A, $C_{24}H_{29}O_9$ |
| 27 | 2060 | 1.3 ± 0.65 | 461.1837 (2) | 461.1817 | +1.99 | 311.1309 | 121.0303/62 | 205.0887/18 | | 3 | 2 | Alnuside B, $C_{24}H_{29}O_9$ |
| 28 | 2090 | 1.3 ± 0.65 | 483.012 (15) | | | 300.99 | 299.9957/13 | | | | 4 | |
| 29 | 2170 | 5.7 ± 2.0 | 447.0964 (100) | 447.0933 | +3.12 | 301.0372/61 | 178.9975/3 | 151.0024/3 | 283.0394/6 | 5 | 2 | Quercitin-rhamnoside, $C_{21}H_{19}O_{11}$ |
| 30 | 2230 | 1.5 ± 0.98 | 359.1517 (1) | 359.1500 | +1.69 | 121.028/100 | 205.08/3 | 327.116/2 | | 3 | 2 | Methylhirsutanonol, $C_{20}H_{23}O_6$ |
| 31 | 2250 | 0.63 ± 1.1 | 445.1866 (1) | 445.1868 | -0.19 | 295.1349/100 | 189.0928/45 | 121.0297/10 | 169.0136/1 | 3 | 2 | platyphylanolanol-xyloside, $C_{24}H_{30}O_8$ |
| 32 | 2298 | 1.0 ± 0.68 | 327.1232 (13) | 327.1238 | -0.60 | 121.031/100 | 205.0896/8 | 109.028/11 | | 3 | 2 | Hirsutanone, $C_{19}H_{19}O_5$ |
| 33 | 2310 | 0.26 ± 0.18 | 485 (0) | | | 255.026/100 | 227.03/66 | 121.027/11 | 327.127/6 | | 4 | |
| 34 | 2380 | 2.7 ± 2.0 | 591.2442 (4) | 591.2447 | -0.50 | 205.086/100 | 327.1282/44 | 121.02/34 | | 4 | 3 | novel diarylheptanoid***, $C_{30}H_{39}O_{12}$ |
| 35 | 2405 | 0.45 ± 0.62 | 561.2274(7) | 561.2341 | -1.44 | 205.0897/100 | 121/48 | 327.1274/32 | 109.029/9 | 4 | 2 | Alnuside C, $C_{29}H_{37}O_{11}$ |

References: 1: (Moilanen et al. 2013), 2: (Gu et al. 2013), 3: (Novakavic et al. 2014), 4: (Lv and Shea 2010), 5. (Falcao et al. 2012) 6. (Sumner et al. 2007)

*HOG: 1,7-bis(3,4-dihydroxyphenyl)-5-β-D-xylopyranosyl-3-heptanone

**Oregonin: 1,7-bis(3,4-dihydroxyphenyl)-5-β-D-glycopyranosyl-3-heptanone

*** Novel diarylheptanoid: Alnuside C with glucose replacing xylose, 1,7-bis-(3,4-dihydroxy-phenyl)-5-hydroxy-3-heptanone-5-0-[2-(2-methylbutenoyl)]-β-D-glucopyranoside

## ELECTRONIC SUPPLEMENTARY MATERIALS

**Fig. S3**. Community similarity illustrated using the phylogenetic distance metrics, (A) unweighted and (B) weighted UNIFRAC. Communities taxonomically described using 16S rRNA marker gene surveys cluster in principal component space by habitat riparian soil, river water, and leaves either taken directly from riparian red alder trees, or from red alder leaf packs submerged underwater on the streambed. All groups differ significantly from each other all pairwise ANOSIMs $p < 0.01$. (C) Further, we describe the relative abundance of bacterial taxa in summary tables for each environment. Despite containing thousands of rare taxa, environmental samples were dominated by relatively few particularly abundant taxa. Among aquatic leaves, note the decline in Comamonadaceae over time. In contrast to the community inhabiting these leaves, the adjacent water column samples remain largely stable over time. The first column shows the relative abundance in the water column, and the second column show the relative abundance on leaves. Taxa included in this table comprised at least 1% of the bacterial community averaged across all leaf packs samples for the noted time point.

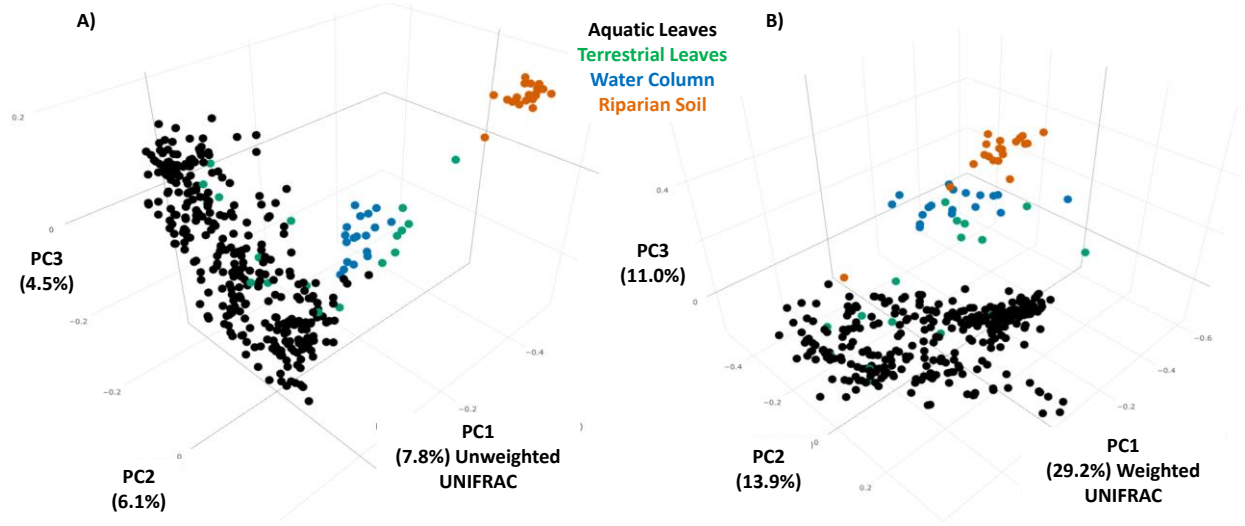

(C)

WATER COLUMN

| Day: 0 | Percent Community Composition of Bacterial Taxa |
|---|---|
| 25.7% | k__Bacteria;p__Actinobacteria;c__Actinobacteria;o__Actinomycetales;f__Microbacteriaceae |
| 20.2% | k__Bacteria;p__Bacteroidetes;c__Flavobacteriia;o__Flavobacteriales;f__Flavobacteriaceae;g__Flavobacterium |
| 15.1% | k__Bacteria;p__Proteobacteria;c__Betaproteobacteria;o__Burkholderiales;f__Comamonadaceae |
| 11.2% | k__Bacteria;p__Bacteroidetes;c__Cytophagia;o__Cytophagales;f__Cytophagaceae |
| 6.5% | k__Bacteria;p__Proteobacteria;c__Betaproteobacteria;o__Burkholderiales;f__Comamonadaceae;Other |
| **Day: 5** | |
| 25.5% | k__Bacteria;p__Actinobacteria;c__Actinobacteria;o__Actinomycetales;f__Microbacteriaceae |
| 15.2% | k__Bacteria;p__Bacteroidetes;c__Flavobacteriia;o__Flavobacteriales;f__Flavobacteriaceae;g__Flavobacterium |
| 14.8% | k__Bacteria;p__Proteobacteria;c__Betaproteobacteria;o__Burkholderiales;f__Comamonadaceae |
| 14.5% | k__Bacteria;p__Bacteroidetes;c__Cytophagia;o__Cytophagales;f__Cytophagaceae |
| 5.4% | k__Bacteria;p__Proteobacteria;c__Betaproteobacteria;o__Burkholderiales;f__Comamonadaceae;Other |
| 5.4% | k__Bacteria;p__Bacteroidetes;c__Flavobacteriia;o__Flavobacteriales;f__Cryomorphaceae;g__Fluviicola |
| **Day: 10** | |
| 28.7% | k__Bacteria;p__Actinobacteria;c__Actinobacteria;o__Actinomycetales;f__Microbacteriaceae |
| 15.7% | k__Bacteria;p__Proteobacteria;c__Betaproteobacteria;o__Burkholderiales;f__Comamonadaceae |
| 14.4% | k__Bacteria;p__Bacteroidetes;c__Flavobacteriia;o__Flavobacteriales;f__Flavobacteriaceae;g__Flavobacterium |
| 9.4% | k__Bacteria;p__Bacteroidetes;c__Cytophagia;o__Cytophagales;f__Cytophagaceae |
| 5.7% | k__Bacteria;p__Proteobacteria;c__Betaproteobacteria;o__Burkholderiales;f__Comamonadaceae;Other |
| **Day: 15** | |
| 30.4% | k__Bacteria;p__Actinobacteria;c__Actinobacteria;o__Actinomycetales;f__Microbacteriaceae |
| 14.7% | k__Bacteria;p__Proteobacteria;c__Betaproteobacteria;o__Burkholderiales;f__Comamonadaceae |
| 11.9% | k__Bacteria;p__Proteobacteria;c__Betaproteobacteria;o__Burkholderiales;f__Comamonadaceae;Other |
| 10.1% | k__Bacteria;p__Bacteroidetes;c__Flavobacteriia;o__Flavobacteriales;f__Flavobacteriaceae;g__Flavobacterium |
| 8.2% | k__Bacteria;p__Bacteroidetes;c__Cytophagia;o__Cytophagales;f__Cytophagaceae |
| **Day: 20** | |
| 38.2% | k__Bacteria;p__Actinobacteria;c__Actinobacteria;o__Actinomycetales;f__Microbacteriaceae |
| 14.5% | k__Bacteria;p__Proteobacteria;c__Betaproteobacteria;o__Burkholderiales;f__Comamonadaceae |
| 9.9% | k__Bacteria;p__Bacteroidetes;c__Flavobacteriia;o__Flavobacteriales;f__Flavobacteriaceae;g__Flavobacterium |
| 7.0% | k__Bacteria;p__Bacteroidetes;c__Cytophagia;o__Cytophagales;f__Cytophagaceae |
| 5.3% | k__Bacteria;p__Proteobacteria;c__Betaproteobacteria;o__Burkholderiales;f__Comamonadaceae;Other |
| 5.0% | k__Bacteria;p__Actinobacteria;c__Actinobacteria;o__Actinomycetales;f__Microbacteriaceae;g__Candidatus Rhodoluna |

SOIL

| | Percent Community Composition of Bacterial Taxa |
|---|---|
| 4.1% | k__Bacteria;p__Proteobacteria;c__Deltaproteobacteria;o__Myxococcales |
| 4.0% | k__Bacteria;p__Proteobacteria;c__Alphaproteobacteria;o__Rhizobiales;f__Hyphomicrobiaceae;g__Rhodoplanes |
| 3.2% | k__Bacteria;p__Proteobacteria;c__Gammaproteobacteria;o__Xanthomonadales;f__Sinobacteraceae |
| 3.1% | k__Bacteria;p__Acidobacteria;c__Acidobacteria-6;o__iii1-15 |
| 3.1% | k__Bacteria;p__Bacteroidetes;c__[Saprospirae];o__[Saprospirales];f__Chitinophagaceae |
| 2.6% | k__Bacteria;p__Proteobacteria;c__Alphaproteobacteria;o__Rhizobiales;f__Bradyrhizobiaceae |
| 2.1% | k__Bacteria;p__Proteobacteria;c__Betaproteobacteria |
| 2.1% | k__Bacteria;p__Acidobacteria;c__Acidobacteriia;o__Acidobacteriales;f__Koribacteraceae |
| 1.9% | k__Bacteria;p__Acidobacteria;c__DA052;o__Ellin6513 |
| 1.9% | k__Bacteria;p__Proteobacteria;c__Alphaproteobacteria;o__Rhodospirillales;f__Rhodospirillaceae |
| 1.8% | k__Bacteria;p__Acidobacteria;c__Solibacteres;o__Solibacterales |
| 1.8% | k__Bacteria;p__Proteobacteria;c__Betaproteobacteria;o__Burkholderiales;f__Comamonadaceae |

TERRESTRIAL LEAVES

| | Percent Community Composition of Bacterial Taxa |
|---|---|
| 12.2% | k__Bacteria;p__Proteobacteria;c__Betaproteobacteria;o__Burkholderiales;f__Comamonadaceae |
| 3.6% | k__Bacteria;p__Proteobacteria;c__Gammaproteobacteria;o__Alteromonadales;f__Alteromonadaceae |
| 3.3% | k__Bacteria;p__Bacteroidetes;c__Bacteroidia;o__Bacteroidales;f__Bacteroidaceae;g__Bacteroides |
| 3.3% | k__Bacteria;p__Bacteroidetes;c__Cytophagia;o__Cytophagales;f__Cytophagaceae;g__Flectobacillus |
| 2.8% | k__Bacteria;p__Proteobacteria;c__Alphaproteobacteria;o__Rhizobiales;f__Rhizobiaceae;g__Agrobacterium |
| 2.7% | k__Bacteria;p__Proteobacteria;c__Alphaproteobacteria;o__Sphingomonadales;f__Sphingomonadaceae;g__Novosphingobium |
| 2.6% | k__Bacteria;p__Proteobacteria;c__Alphaproteobacteria;o__Rhodobacterales;f__Rhodobacteraceae;g__Rhodobacter |
| 2.5% | k__Bacteria;p__Proteobacteria;c__Betaproteobacteria;o__Burkholderiales;f__Comamonadaceae;Other |
| 2.4% | k__Bacteria;p__Tenericutes;c__Mollicutes;o__Acholeplasmatales;f__Acholeplasmataceae;g__Candidatus Phytoplasma |
| 2.1% | k__Bacteria;p__Proteobacteria;c__Alphaproteobacteria;o__Sphingomonadales;f__Sphingomonadaceae |
| 2.0% | k__Bacteria;p__Proteobacteria;c__Deltaproteobacteria;o__Myxococcales |
| 1.9% | k__Bacteria;p__Proteobacteria;c__Alphaproteobacteria;o__Rhodobacterales;f__Rhodobacteraceae |

AQUATIC LEAVES

| Day: 5 | | Percent Community Composition of Bacterial Taxa |
|---|---|---|
| Water Column | Leaves | |
| 20.2% | 54.7% | k__Bacteria;p__Proteobacteria;c__Betaproteobacteria;o__Burkholderiales;f__Comamonadaceae |
| 0.1% | 5.7% | k__Bacteria;p__Proteobacteria;c__Alphaproteobacteria;o__Sphingomonadales;f__Sphingomonadaceae;g__Novosphingobium |
| 0.1% | 3.4% | k__Bacteria;p__Proteobacteria;c__Deltaproteobacteria;o__Myxococcales |
| 0.6% | 3.0% | k__Bacteria;p__Proteobacteria;c__Alphaproteobacteria;o__Rhodobacterales;f__Rhodobacteraceae;g__Rhodobacter |
| 0.05% | 2.1% | k__Bacteria;p__Bacteroidetes;c__Cytophagia;o__Cytophagales;f__Cytophagaceae;g__Flectobacillus |
| 0.02% | 1.8% | k__Bacteria;p__Proteobacteria;c__Alphaproteobacteria;o__Sphingomonadales;f__Sphingomonadaceae |
| 0.05% | 1.6% | k__Bacteria;p__Proteobacteria;c__Betaproteobacteria;o__Burkholderiales;f__Comamonadaceae;g__Leptothrix |
| 0.01% | 1.5% | k__Bacteria;p__Proteobacteria;c__Gammaproteobacteria;o__Pseudomonadales;f__Moraxellaceae |
| 15.2% | 1.4% | k__Bacteria;p__Bacteroidetes;c__Flavobacteriia;o__Flavobacteriales;f__Flavobacteriaceae;g__Flavobacterium |
| 0.04% | 1.3% | k__Bacteria;p__Proteobacteria;c__Alphaproteobacteria;o__Rhizobiales;f__Rhizobiaceae;g__Agrobacterium |
| 0.01% | 1.1% | k__Bacteria;p__Proteobacteria;c__Alphaproteobacteria;o__Rhizobiales |
| **Day: 10** | | |
| 21.4% | 34.1% | k__Bacteria;p__Proteobacteria;c__Betaproteobacteria;o__Burkholderiales;f__Comamonadaceae |
| 0.2% | 14.7% | k__Bacteria;p__Proteobacteria;c__Deltaproteobacteria;o__Myxococcales |
| 0.1% | 7.0% | k__Bacteria;p__Proteobacteria;c__Alphaproteobacteria;o__Sphingomonadales;f__Sphingomonadaceae;g__Novosphingobium |
| 0.7% | 4.2% | k__Bacteria;p__Proteobacteria;c__Alphaproteobacteria;o__Rhodobacterales;f__Rhodobacteraceae;g__Rhodobacter |
| 0.2% | 3.7% | k__Bacteria;p__Proteobacteria;c__Alphaproteobacteria;o__Sphingomonadales;f__Sphingomonadaceae |
| 0.04% | 2.7% | k__Bacteria;p__Bacteroidetes;c__Cytophagia;o__Cytophagales;f__Cytophagaceae;g__Flectobacillus |
| 14.4% | 1.9% | k__Bacteria;p__Bacteroidetes;c__Flavobacteriia;o__Flavobacteriales;f__Flavobacteriaceae;g__Flavobacterium |
| 0.04% | 1.9% | k__Bacteria;p__Proteobacteria;c__Alphaproteobacteria;o__Rhizobiales;f__Rhizobiaceae;g__Agrobacterium |
| 0.2% | 1.5% | k__Bacteria;p__Proteobacteria;c__Betaproteobacteria;o__Burkholderiales;f__Oxalobacteraceae |
| 0.3% | 1.4% | k__Bacteria;p__Proteobacteria;c__Alphaproteobacteria;o__Rhizobiales |
| 0.2% | 1.3% | k__Bacteria;p__Proteobacteria;c__Gammaproteobacteria;o__Enterobacteriales;f__Enterobacteriaceae;Other |
| 0.1% | 1.2% | k__Bacteria;p__Proteobacteria;c__Betaproteobacteria;o__Methylophilales;f__Methylophilaceae;g__Methylotenera |
| 0.3% | 1.1% | k__Bacteria;p__Bacteroidetes;c__Saprospirae;o__Saprospirales;f__Chitinophagaceae |
| 0.5% | 1.0% | k__Bacteria;p__Proteobacteria;c__Alphaproteobacteria;o__Sphingomonadales |
| **Day: 15** | | |
| 26.6% | 25.9% | k__Bacteria;p__Proteobacteria;c__Betaproteobacteria;o__Burkholderiales;f__Comamonadaceae |
| 0.1% | 7.6% | k__Bacteria;p__Proteobacteria;c__Deltaproteobacteria;o__Myxococcales |
| 0.05% | 5.5% | k__Bacteria;p__Bacteroidetes;c__Cytophagia;o__Cytophagales;f__Cytophagaceae;g__Flectobacillus |
| 1.1% | 5.5% | k__Bacteria;p__Proteobacteria;c__Alphaproteobacteria;o__Rhodobacterales;f__Rhodobacteraceae;g__Rhodobacter |
| 0.2% | 5.4% | k__Bacteria;p__Proteobacteria;c__Alphaproteobacteria;o__Sphingomonadales;f__Sphingomonadaceae;g__Novosphingobium |
| 0.2% | 5.0% | k__Bacteria;p__Proteobacteria;c__Alphaproteobacteria;o__Sphingomonadales;f__Sphingomonadaceae |
| 0.03% | 3.8% | k__Bacteria;p__Proteobacteria;c__Alphaproteobacteria;o__Rhizobiales;f__Rhizobiaceae;g__Agrobacterium |
| 10.1% | 3.4% | k__Bacteria;p__Bacteroidetes;c__Flavobacteriia;o__Flavobacteriales;f__Flavobacteriaceae;g__Flavobacterium |
| 0.3% | 2.9% | k__Bacteria;p__Proteobacteria;c__Alphaproteobacteria;o__Rhizobiales |
| 0.3% | 2.1% | k__Bacteria;p__Bacteroidetes;c__Saprospirae;o__Saprospirales;f__Chitinophagaceae |
| 0.01% | 2.0% | k__Bacteria;p__Proteobacteria;c__Alphaproteobacteria;o__Caulobacterales;f__Caulobacteraceae;g__Asticcacaulis |
| 0.1% | 1.9% | k__Bacteria;p__Proteobacteria;c__Betaproteobacteria;o__Methylophilales;f__Methylophilaceae;g__Methylotenera |
| 0.2% | 1.5% | k__Bacteria;p__Proteobacteria;c__Betaproteobacteria;o__Burkholderiales;f__Oxalobacteraceae |
| 0.4% | 1.4% | k__Bacteria;p__Proteobacteria;c__Alphaproteobacteria;o__Sphingomonadales |
| 0.1% | 1.3% | k__Bacteria;p__Proteobacteria;c__Alphaproteobacteria;o__Caulobacterales;f__Caulobacteraceae |
| 0.1% | 1.1% | k__Bacteria;p__Proteobacteria;c__Betaproteobacteria;o__Methylophilales;f__Methylophilaceae |
| **Day: 20** | | |
| 19.8% | 21.8% | k__Bacteria;p__Proteobacteria;c__Betaproteobacteria;o__Burkholderiales;f__Comamonadaceae |
| 9.9% | 6.3% | k__Bacteria;p__Bacteroidetes;c__Flavobacteriia;o__Flavobacteriales;f__Flavobacteriaceae;g__Flavobacterium |
| 0.03% | 5.1% | k__Bacteria;p__Bacteroidetes;c__Cytophagia;o__Cytophagales;f__Cytophagaceae;g__Flectobacillus |
| 0.05% | 4.8% | k__Bacteria;p__Proteobacteria;c__Alphaproteobacteria;o__Rhizobiales;f__Rhizobiaceae;g__Agrobacterium |
| 0.5% | 4.7% | k__Bacteria;p__Proteobacteria;c__Alphaproteobacteria;o__Rhodobacterales;f__Rhodobacteraceae;g__Rhodobacter |
| 0.4% | 4.0% | k__Bacteria;p__Proteobacteria;c__Alphaproteobacteria;o__Rhizobiales |
| 0.2% | 3.8% | k__Bacteria;p__Proteobacteria;c__Alphaproteobacteria;o__Sphingomonadales;f__Sphingomonadaceae |
| 0.1% | 3.7% | k__Bacteria;p__Proteobacteria;c__Alphaproteobacteria;o__Sphingomonadales;f__Sphingomonadaceae;g__Novosphingobium |
| 0.3% | 3.4% | k__Bacteria;p__Bacteroidetes;c__Saprospirae;o__Saprospirales;f__Chitinophagaceae |
| 0.1% | 3.2% | k__Bacteria;p__Proteobacteria;c__Deltaproteobacteria;o__Myxococcales |
| 0.1% | 2.7% | k__Bacteria;p__Proteobacteria;c__Betaproteobacteria;o__Methylophilales;f__Methylophilaceae;g__Methylotenera |
| 0.02% | 2.1% | k__Bacteria;p__Proteobacteria;c__Alphaproteobacteria;o__Caulobacterales;f__Caulobacteraceae;g__Asticcacaulis |
| 0.1% | 1.6% | k__Bacteria;p__Proteobacteria;c__Alphaproteobacteria;o__Caulobacterales;f__Caulobacteraceae |
| 0.1% | 1.6% | k__Bacteria;p__Proteobacteria;c__Betaproteobacteria;o__Burkholderiales;f__Oxalobacteraceae |
| 0.00% | 1.5% | k__Bacteria;p__Bacteroidetes;c__Cytophagia;o__Cytophagales;f__Cytophagaceae;g__Emticicia |
| 0.6% | 1.5% | k__Bacteria;p__Proteobacteria;c__Alphaproteobacteria;o__Sphingomonadales |
| 0.1% | 1.3% | k__Bacteria;p__Proteobacteria;c__Betaproteobacteria;o__Burkholderiales;f__Comamonadaceae;g__Rubrivivax |
| 0.1% | 1.1% | k__Bacteria;p__Proteobacteria;c__Alphaproteobacteria;o__Rhizobiales;f__Phyllobacteriaceae |
| 0.1% | 1.1% | k__Bacteria;p__Proteobacteria;c__Alphaproteobacteria;o__Rhizobiales;f__Hyphomicrobiaceae;g__Devosia |
| 0.05% | 1.0% | k__Bacteria;p__Proteobacteria;c__Betaproteobacteria;o__Methylophilales;f__Methylophilaceae |

## ELECTRONIC SUPPLEMENTARY MATERIALS

**Fig. S4.** Bacteria inhabiting red alder leaf packs submerged on riverbeds are derived more so from (A) terrestrial leaves (estimated 66.7 ± 0.9 s.e. %) and (B) unknown sources (29.6 ± 0.9 %), while the water column and riparian soil are not shown as they were more minor contributors (2.9 ± 0.1 % and 0.82 ± 0.04 %, respectively) to the bacterial community according to Bayesian SourceTracker models. Proportions of the bacterial community derived from terrestrial leaves varied significantly by days of incubation and leaf origin, however effects were incubation site specific. Panels indicate site of incubation. Note that all points are horizontally jittered to minimize overplotting.

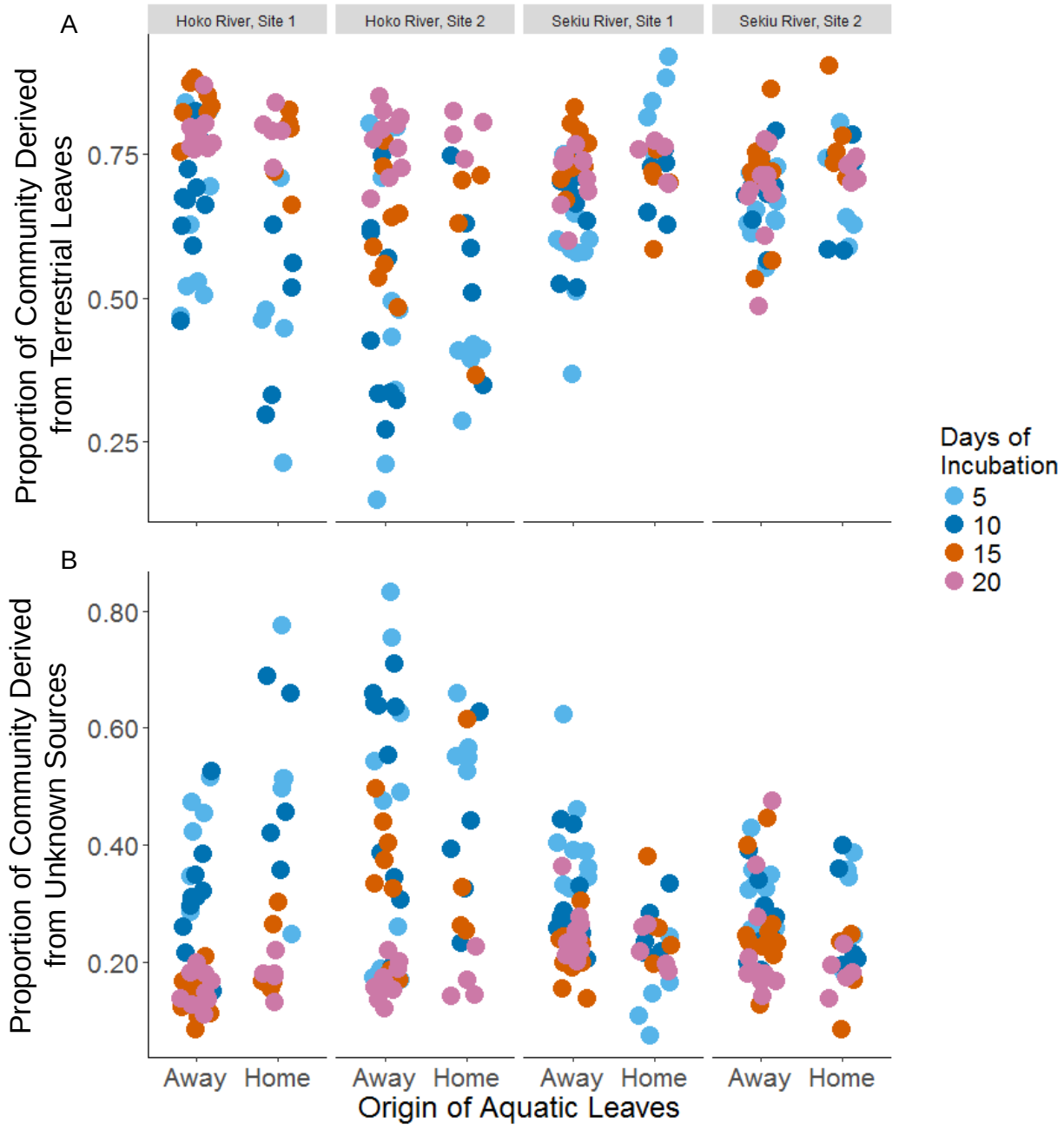

## ELECTRONIC SUPPLEMENTARY MATERIALS

**Fig. S5.** Certain taxa inhabiting decomposing alder leaf litter varied significantly in relative abundance over time. (A) We characterized each taxon as early, mid, or late successional based on visual inspection of relative abundance plots, as shown below. We defined early-stage taxa as those with highest relative abundance during day 5, mid-stage as those with highest relative abundance during day 10 and 15, and late stage taxa as those with highest relative abundance during day 20. We restricted this analysis to 91 taxa that comprised at least 1% of the community in at least one sample. Instead of averaging across our sample set, this approach included taxa that may comprise a sizable portion of a community, but only in a subset of samples. (B) We also summarize these results in a table where all reported significance values were corrected for multiple comparisons testing using the false discovery rate correction. We also note taxa with significant day x site interactions, as well as taxa with significant day x leaf origin and day x leaf origin x site interactions to identify taxa that may be contributing to accelerated decomposition of local leaves. Only a single taxon in the order Pedosphaerales showed a significant day x leaf origin interactions.

(A)

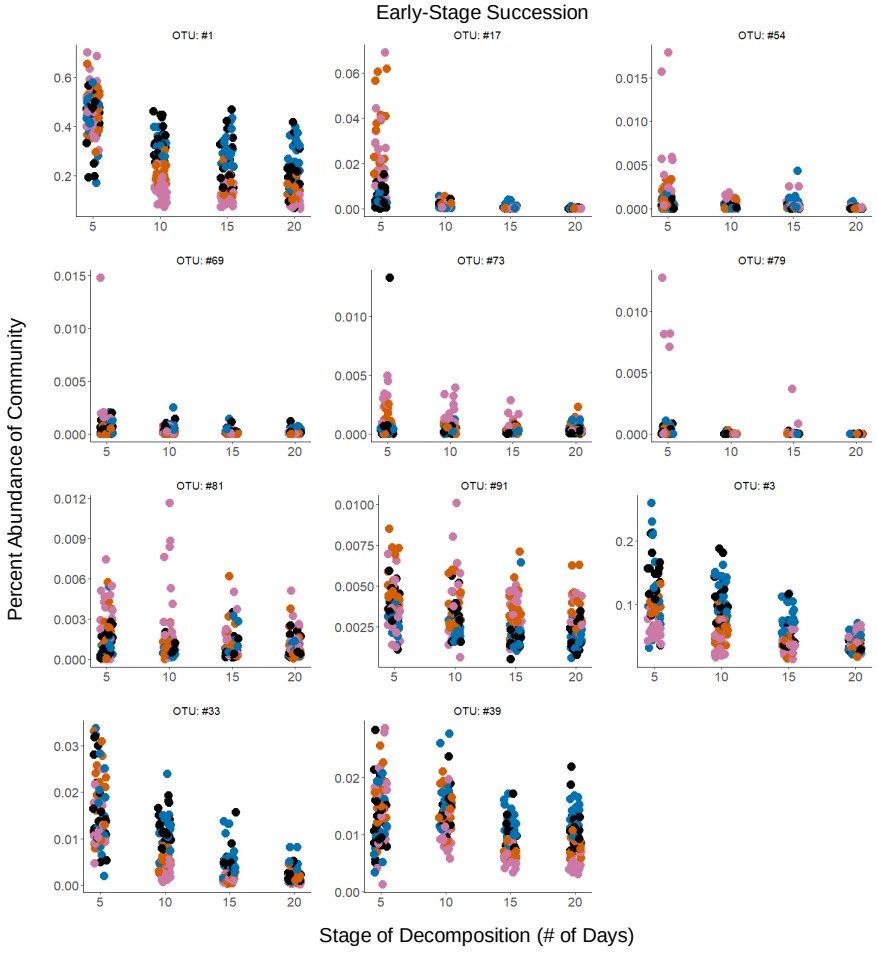

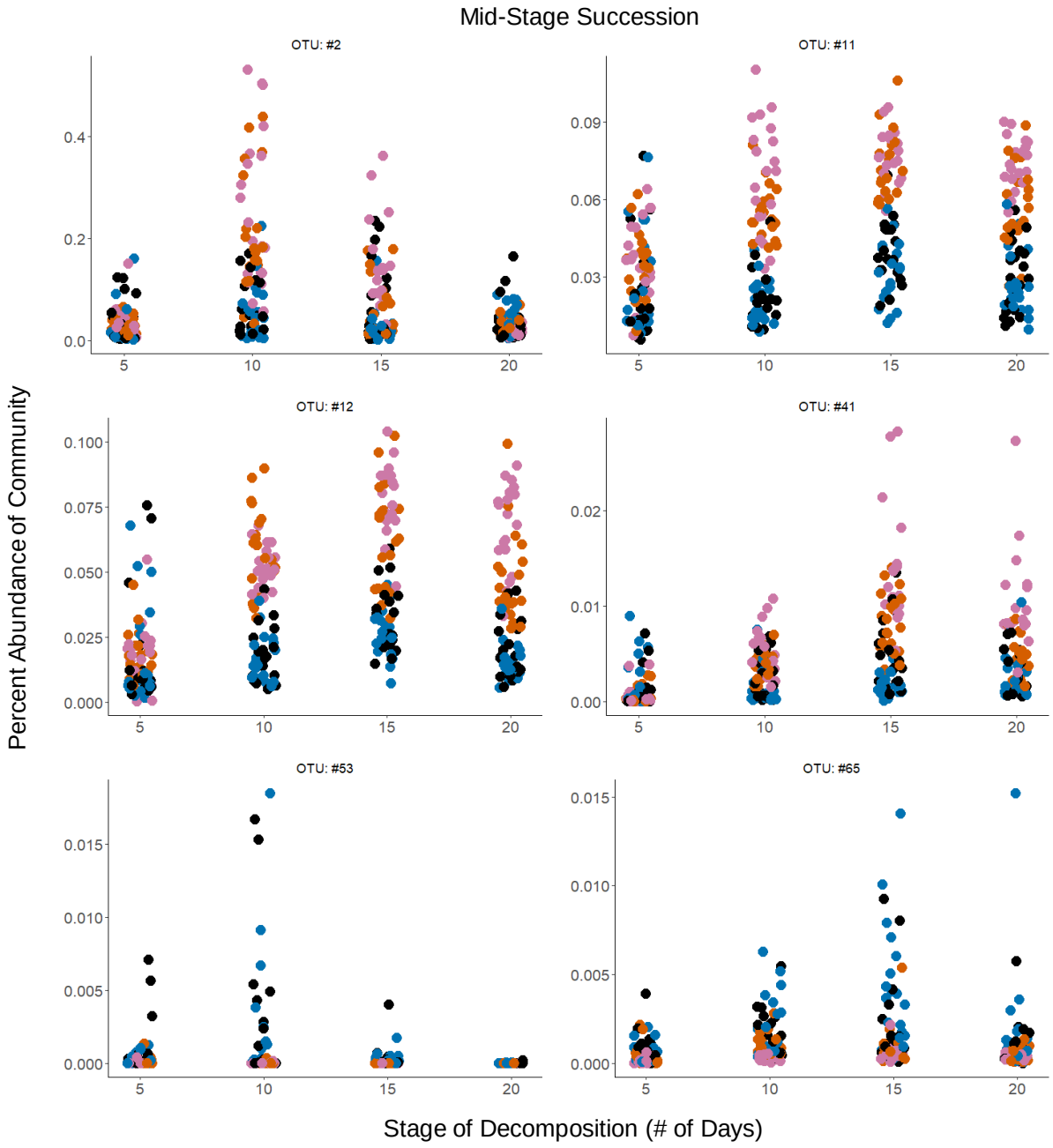
Mid-Stage Succession
OTU: #2
OTU: #11
OTU: #12
OTU: #41
OTU: #53
OTU: #65
Percent Abundance of Community
Stage of Decomposition (# of Days)

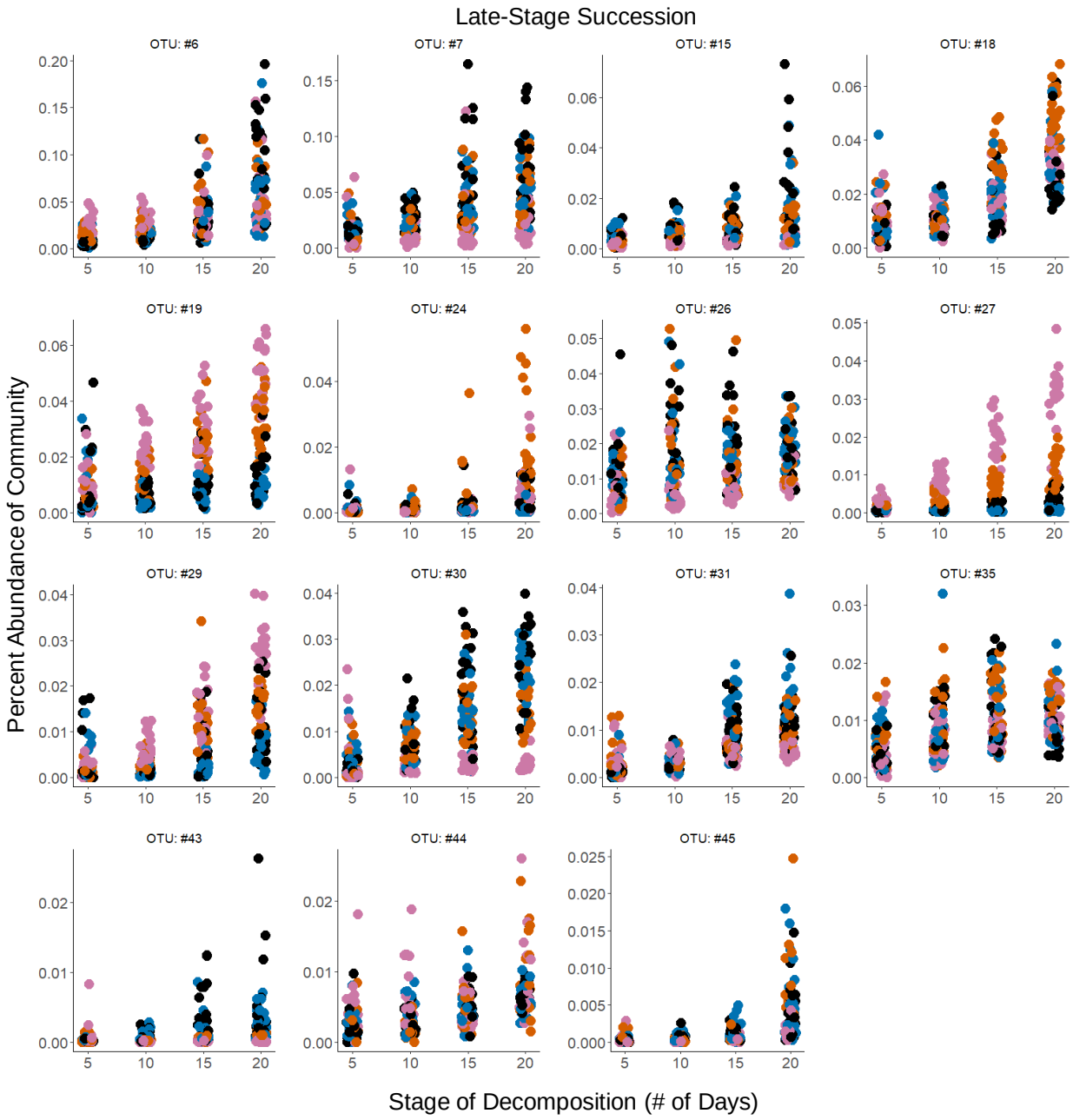
Late-Stage Succession
OTU: #6
OTU: #7
OTU: #15
OTU: #18
OTU: #19
OTU: #24
OTU: #26
OTU: #27
OTU: #29
OTU: #30
OTU: #31
OTU: #35
OTU: #43
OTU: #44
OTU: #45
Percent Abundance of Community
Stage of Decomposition (# of Days)

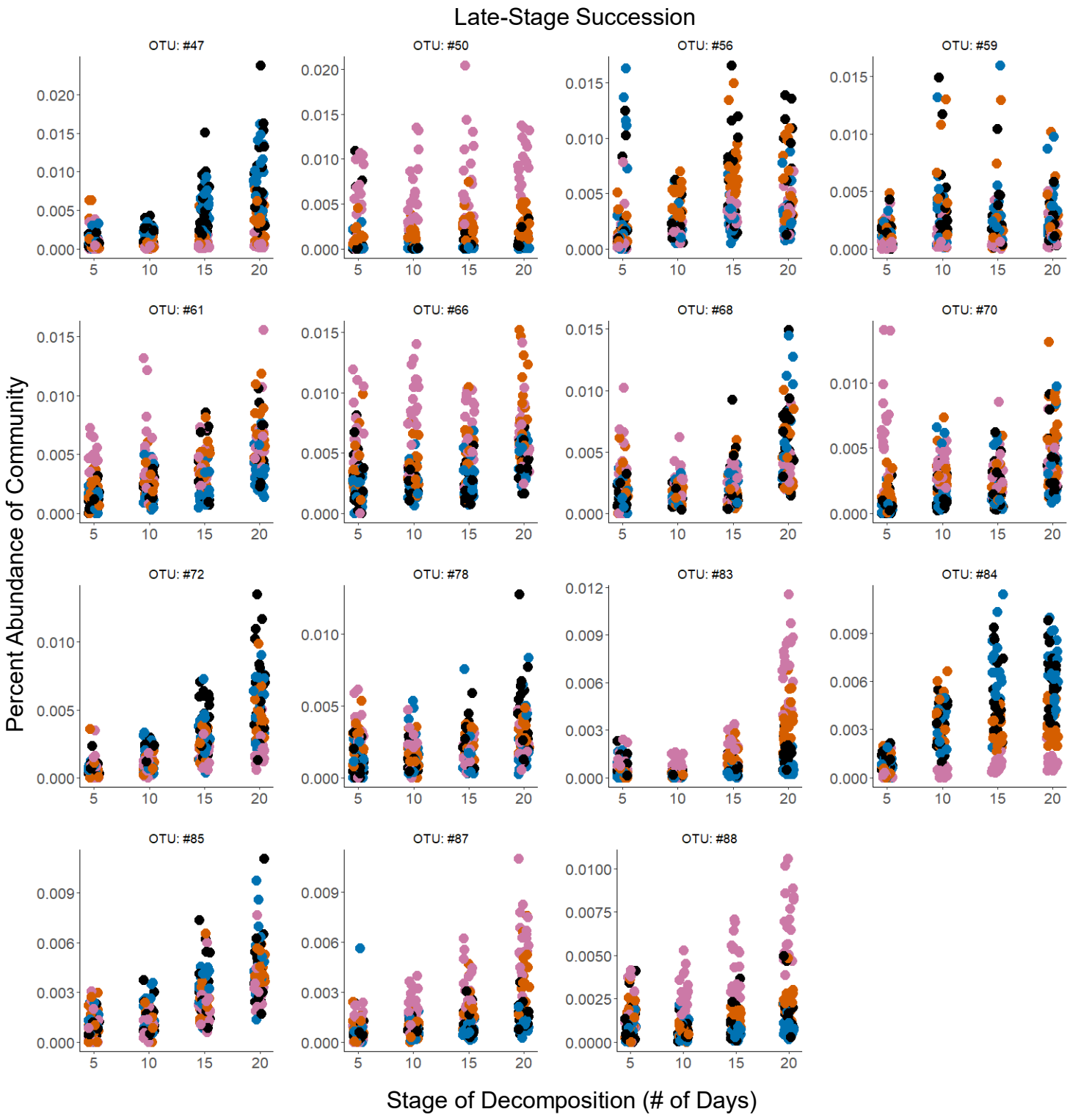
Late-Stage Succession
OTU: #47
OTU: #50
OTU: #56
OTU: #59
OTU: #61
OTU: #66
OTU: #68
OTU: #70
OTU: #72
OTU: #78
OTU: #83
OTU: #84
OTU: #85
OTU: #87
OTU: #88
Percent Abundance of Community
Stage of Decomposition (# of Days)

(B)

**Taxa Significantly Characteristic of Early-Stage Succession**

| OTU | OTU # | $F_{3,295}$ | p-value | $R^2$ |
|---|---|---|---|---|
| k__Bacteria;p__Proteobacteria;c__Betaproteobacteria;o__Burkholderiales;f__Comamonadaceae | 1 | 194.0 | 1.6E-67 | 0.52 |
| k__Bacteria;p__Proteobacteria;c__Betaproteobacteria;o__Burkholderiales;f__Comamonadaceae;Other | 3 | 94.9 | 4.5E-41 | 0.33 |
| k__Bacteria;p__Proteobacteria;c__Gammaproteobacteria;o__Pseudomonadales;f__Moraxellaceae | 17 | 105.7 | 1.6E-44 | 0.35 |
| k__Bacteria;p__Proteobacteria;c__Betaproteobacteria;o__Burkholderiales;f__Comamonadaceae;g__Leptothrix | 33 | 173.6 | 6.9E-63 | 0.55 |
| Unassigned;Other;Other;Other;Other;Other | 39 | 43.6 | 2.1E-21 | 0.24 |
| k__Bacteria;p__Proteobacteria;c__Gammaproteobacteria;o__Pseudomonadales;f__Moraxellaceae;g__Acinetobacter | 54 | 16.2 | 7.8E-08 | 0.11 |
| k__Bacteria;p__Cyanobacteria;c__Oscillatoriophycideae;o__Oscillatoriales;f__Phormidiaceae;g__Phormidium | 69 | 6.1 | 4.6E-02 | 0.04 |
| k__Bacteria;p__Verrucomicrobia;c__Pedosphaerae;o__Pedosphaerales;f__R4-41B | 73 | 9.9 | 2.8E-04 | 0.07 |
| k__Bacteria;p__Bacteroidetes;c__Bacteroidia;o__Bacteroidales;f__S24-7;g__ | 79 | 6.1 | 4.3E-02 | 0.04 |
| k__Bacteria;p__Proteobacteria;c__Alphaproteobacteria;o__Sphingomonadales;f__Sphingomonadaceae;g__Zymomonas | 81 | 6.4 | 2.8E-02 | 0.04 |
| k__Bacteria;p__Proteobacteria;c__Betaproteobacteria;o__Burkholderiales;f__Comamonadaceae;g__Methylibium | 91 | 13.4 | 2.8E-06 | 0.09 |

**Taxa Significantly Characteristic of Mid-Stage Succession**

| OTU | OTU # | $F_{3,295}$ | p-value | $R^2$ |
|---|---|---|---|---|
| k__Bacteria;p__Proteobacteria;c__Deltaproteobacteria;o__Myxococcales;f__;g__ | 2 | 53.5 | 1.20E-25 | 0.24 |
| k__Bacteria;p__Proteobacteria;c__Alphaproteobacteria;o__Rhodobacterales;f__Rhodobacteraceae;g__Rhodobacter | 11 | 44.7 | 7.20E-22 | 0.13 |
| k__Bacteria;p__Proteobacteria;c__Alphaproteobacteria;o__Sphingomonadales;f__Sphingomonadaceae | 12 | 71.6 | 7.30E-33 | 0.21 |
| k__Bacteria;p__Proteobacteria;c__Alphaproteobacteria;o__Sphingomonadales;f__Sphingomonadaceae;g__Sphingobium | 41 | 58.9 | 6.60E-28 | 0.23 |
| k__Bacteria;p__Proteobacteria;c__Epsilonproteobacteria;o__Campylobacterales;f__Campylobacteraceae;g__Arcobacter | 53 | 8.2 | 2.60E-03 | 0.06 |
| k__Bacteria;p__Proteobacteria;c__Alphaproteobacteria;o__Sphingomonadales;Other;Other | 65 | 9.6 | 4.00E-04 | 0.06 |

**Taxa Significantly Characteristic of Late-Stage Succession**

| OTU | OTU # | $F_{3,295}$ | p-value | $R^2$ |
|---|---|---|---|---|
| k__Bacteria;p__Bacteroidetes;c__Flavobacteriia;o__Flavobacteriales;f__Flavobacteriaceae;g__Flavobacterium | 6 | 64.4 | 4.30E-30 | 0.35 |
| k__Bacteria;p__Proteobacteria;c__Alphaproteobacteria;o__Rhizobiales;f__Rhizobiaceae;g__Agrobacterium | 7 | 50.8 | 1.6E-24 | 0.26 |
| k__Bacteria;p__Proteobacteria;c__Betaproteobacteria;o__Burkholderiales;f__Comamonadaceae;g__Rubrivivax | 15 | 25.7 | 7.6E-13 | 0.16 |
| k__Bacteria;p__Bacteroidetes;c__Saprospirae;o__Saprospirales;f__Chitinophagaceae | 18 | 165.8 | 4.9E-61 | 0.53 |
| k__Bacteria;p__Proteobacteria;c__Betaproteobacteria;o__Methylophilales;f__Methylophilaceae;g__Methylotenera | 19 | 96.7 | 1.2E-41 | 0.25 |
| k__Bacteria;p__Actinobacteria;c__Actinobacteria;o__Actinomycetales;f__Micromonosporaceae;g__Actinoplanes | 24 | 35.8 | 8.3E-18 | 0.19 |
| k__Bacteria;p__Proteobacteria;c__Betaproteobacteria;o__Burkholderiales;f__Oxalobacteraceae | 26 | 10.4 | 1.4E-04 | 0.07 |
| k__Bacteria;p__Proteobacteria;c__Alphaproteobacteria;o__Rhizobiales;f__Phyllobacteriaceae | 27 | 170.2 | 4.5E-62 | 0.18 |
| k__Bacteria;p__Bacteroidetes;c__Cytophagia;o__Cytophagales;f__Cytophagaceae;g__Emticicia | 29 | 126.4 | 1.0E-50 | 0.38 |
| k__Bacteria;p__Proteobacteria;c__Alphaproteobacteria;o__Caulobacterales;f__Caulobacteraceae | 30 | 109.8 | 8.4E-46 | 0.34 |
| k__Bacteria;p__Proteobacteria;c__Alphaproteobacteria;o__Rhizobiales;f__Hyphomicrobiaceae;g__Devosia | 31 | 98.1 | 4.2E-42 | 0.40 |
| k__Bacteria;p__Proteobacteria;c__Betaproteobacteria;o__Methylophilales;f__Methylophilaceae | 35 | 28.7 | 2.4E-14 | 0.20 |
| k__Bacteria;p__Proteobacteria;c__Deltaproteobacteria;o__MIZ46;f__;g__ | 43 | 16.2 | 7.8E-08 | 0.10 |
| k__Bacteria;p__Verrucomicrobia;c__Verrucomicrobiae;o__Verrucomicrobiales;f__Verrucomicrobiaceae | 44 | 30.1 | 4.8E-15 | 0.20 |
| k__Bacteria;p__Proteobacteria;c__Gammaproteobacteria;o__Xanthomonadales;f__Sinobacteraceae;g__Steroidobacter | 45 | 54.9 | 2.9E-26 | 0.32 |
| k__Bacteria;p__Proteobacteria;c__Alphaproteobacteria;o__Caulobacterales;f__Caulobacteraceae;g__Caulobacter | 47 | 63.0 | 1.6E-29 | 0.24 |
| k__Bacteria;p__Bacteroidetes;c__Cytophagia;o__Cytophagales;f__Cytophagaceae;g__Leadbetterella | 50 | 7.3 | 9.4E-03 | 0.02 |
| k__Bacteria;p__Proteobacteria;c__Alphaproteobacteria;o__Sphingomonadales;f__Sphingomonadaceae;Other | 56 | 19.6 | 1.2E-09 | 0.12 |
| k__Bacteria;p__Proteobacteria;c__Gammaproteobacteria;o__;f__;g__ | 59 | 6.6 | 2.2E-02 | 0.05 |
| k__Bacteria;p__Planctomycetes;c__Planctomycetia;o__Pirellulales;f__Pirellulaceae | 61 | 46.1 | 1.6E-22 | 0.26 |
| k__Bacteria;p__Bacteroidetes;c__Sphingobacteriia;o__Sphingobacteriales | 66 | 19.8 | 9.2E-10 | 0.09 |
| k__Bacteria;p__Bacteroidetes;c__Cytophagia;o__Cytophagales;f__Cytophagaceae | 68 | 64.1 | 5.7E-30 | 0.35 |
| k__Bacteria;p__Bacteroidetes;c__Flavobacteriia;o__Flavobacteriales;f__Cryomorphaceae;g__Fluviicola | 70 | 18.0 | 8.2E-09 | 0.10 |
| k__Bacteria;p__Proteobacteria;c__Alphaproteobacteria;o__Rhodobacterales;f__Hyphomonadaceae | 72 | 126.8 | 8.2E-51 | 0.46 |
| k__Bacteria;p__Bacteroidetes;c__Saprospirae;o__Saprospirales;f__Saprospiraceae | 78 | 15.6 | 1.7E-07 | 0.11 |
| k__Bacteria;p__Acidobacteria;c__Chloracidobacteria;o__RB41;f__Ellin6075 | 83 | 213.4 | 1.3E-71 | 0.36 |
| k__Bacteria;p__Proteobacteria;c__Alphaproteobacteria;o__BD7-3 | 84 | 122.9 | 1.0E-49 | 0.29 |
| k__Bacteria;p__Armatimonadetes;c__Fimbriimonadia;o__Fimbriimonadales;f__Fimbriimonadaceae;g__Fimbriimonas | 85 | 136.9 | 1.3E-53 | 0.54 |
| k__Bacteria;p__Verrucomicrobia;c__partobacteria;o__Chthoniobacterales;f__Chthoniobacteraceae | 87 | 81.1 | 2.5E-36 | 0.25 |
| k__Bacteria;p__Proteobacteria;c__Alphaproteobacteria;o__Rhizobiales;f__Hyphomicrobiaceae;g__Hyphomicrobium | 88 | 41.7 | 1.50E-20 | 0.11 |

**Successional Patterns Signficant but Variable by Incubation Site**

| OTU | OTU # | $F_{3,295}$ | p-value | $R^2$ |
|---|---|---|---|---|
| k__Bacteria;p__Bacteroidetes;c__Cytophagia;o__Cytophagales;f__Cytophagaceae;g__Flectobacillus | 4 | 28.5 | 2.9E-14 | 0.11 |
| k__Bacteria;p__Proteobacteria;c__Alphaproteobacteria;o__Sphingomonadales;f__Sphingomonadaceae;g__Novosphingobium | 5 | 22.1 | 5.9E-11 | 0.14 |
| k__Bacteria;p__Proteobacteria;c__Alphaproteobacteria;o__Rhizobiales | 8 | 139.1 | 3.3E-54 | 0.21 |
| k__Bacteria;p__Proteobacteria;c__Alphaproteobacteria;o__Caulobacterales;f__Caulobacteraceae;g__Asticcacaulis | 10 | 32.0 | 5.9E-16 | 0.14 |
| k__Bacteria;p__Proteobacteria;c__Gammaproteobacteria;o__Aeromonadales;f__Aeromonadaceae;g__Tolumonas | 14 | 12.5 | 9.8E-06 | 0.08 |
| k__Bacteria;p__Proteobacteria;c__Gammaproteobacteria;o__Enterobacteriales;f__Enterobacteriaceae | 20 | 6.6 | 2.2E-02 | 0.04 |
| k__Bacteria;p__Spirochaetes;c__Spirochaetes;o__Spirochaetales;f__Spirochaetaceae;g__Spirochaeta | 21 | 24.6 | 2.8E-12 | 0.10 |
| k__Bacteria;p__Proteobacteria;c__Alphaproteobacteria;o__Rhizobiales;Other;Other | 22 | 35.6 | 1.1E-17 | 0.09 |
| k__Bacteria;p__Proteobacteria;c__Alphaproteobacteria;o__Sphingomonadales | 23 | 36.1 | 6.3E-18 | 0.06 |
| k__Bacteria;p__Bacteroidetes;c__Sphingobacteriia;o__Sphingobacteriales;f__Sphingobacteriaceae | 28 | 12.1 | 1.6E-05 | 0.07 |
| k__Bacteria;p__Proteobacteria;c__Betaproteobacteria;o__Rhodocyclales;f__Rhodocyclaceae;g__Thauera | 32 | 8.2 | 2.6E-03 | 0.05 |
| k__Bacteria;p__Bacteroidetes;c__Saprospirae;o__Saprospirales;f__Chitinophagaceae;g__Chitinophaga | 46 | 21.2 | 1.6E-10 | 0.13 |
| k__Bacteria;p__Bacteroidetes;c__Saprospirae;o__Saprospirales;f__Chitinophagaceae;g__Sediminibacterium | 49 | 14.7 | 5.2E-07 | 0.05 |
| k__Bacteria;p__Proteobacteria;c__Alphaproteobacteria;o__Rhizobiales;f__Rhizobiaceae;Other | 58 | 10.9 | 7.1E-05 | 0.07 |
| k__Bacteria;p__Proteobacteria;c__Betaproteobacteria;o__Burkholderiales;f__Comamonadaceae;g__Limnobacter | 77 | 8.3 | 2.4E-03 | 0.05 |
| k__Bacteria;p__Firmicutes;c__Clostridia;o__Clostridiales;f__Veillonellaceae;g__Pelosinus | 89 | 17.4 | 1.8E-08 | 0.11 |
| k__Bacteria;p__Proteobacteria;c__Betaproteobacteria;o__Neisseriales;f__Neisseriaceae;Other | 90 | 7.5 | 6.9E-03 | 0.04 |

**Significant Day x Site x Leaf Origin Interaction**

| OTU | OTU # | $F_{3,295}$ | p-value | $R^2$ |
|---|---|---|---|---|
| k__Bacteria;p__Proteobacteria;c__Gammaproteobacteria;o__Legionellales;f__Coxiellaceae;g__Rickettsiella | 63 | 5.1 | < 0.001 | 0.01 |
| Unassigned;Other;Other;Other;Other;Other | 39 | 4.9 | < 0.001 | 0.24 |
| k__Bacteria;p__Proteobacteria;c__Betaproteobacteria;o__Burkholderiales;f__Comamonadaceae;Other | 3 | 4.1 | 0.0058 | 0.33 |
| k__Bacteria;p__Proteobacteria;c__Betaproteobacteria;o__Burkholderiales;f__Comamonadaceae;g__Leptothrix | 33 | 3.5 | 0.039 | 0.55 |
| k__Bacteria;p__Proteobacteria;c__Gammaproteobacteria;o__Thiotrichales;f__Thiotrichaceae | 82 | 3.3 | 0.078 | 0.01 |

## ELECTRONIC SUPPLEMENTARY MATERIALS

**Fig. S6**. Packs of leaves derived from riparian red alder trees growing a distance away from the incubation site tended to harbor greater bacterial diversity than leaf packs consisting of leaves from the immediately local riparian zone. A linear mixed model of Faith's Phylogenetic Diversity against leaf origin was conducted on five categories of leaf origin with an ordered-ANOVA correction $r_sP_C$ to test our apriori hypothesis that leaves in the Home categories would differ from leaves in the Away categories. For illustration, we show this condensed contrast of Home versus Away that includes all five leaf origin categories reduced to two. Alpha diversity metrics are shown here as standardized scores (i.e., z-scores), in which diversity measures within an incubation site and by each day are adjusted to a $\mu = 0$, s.d. = 1, so a y-axis value = 1 indicates 1 s.d. above the mean alpha diversity measurement for that incubation site from that day. This standardization serves to illustrate the relative diversity measures of the Home versus Away leaf communities, however the mixed-effects model was run on the non-standardized data with day as a fixed effect, and incubation site and tree identity as a random effect. Note points are horizontally jittered to minimize overplotting.

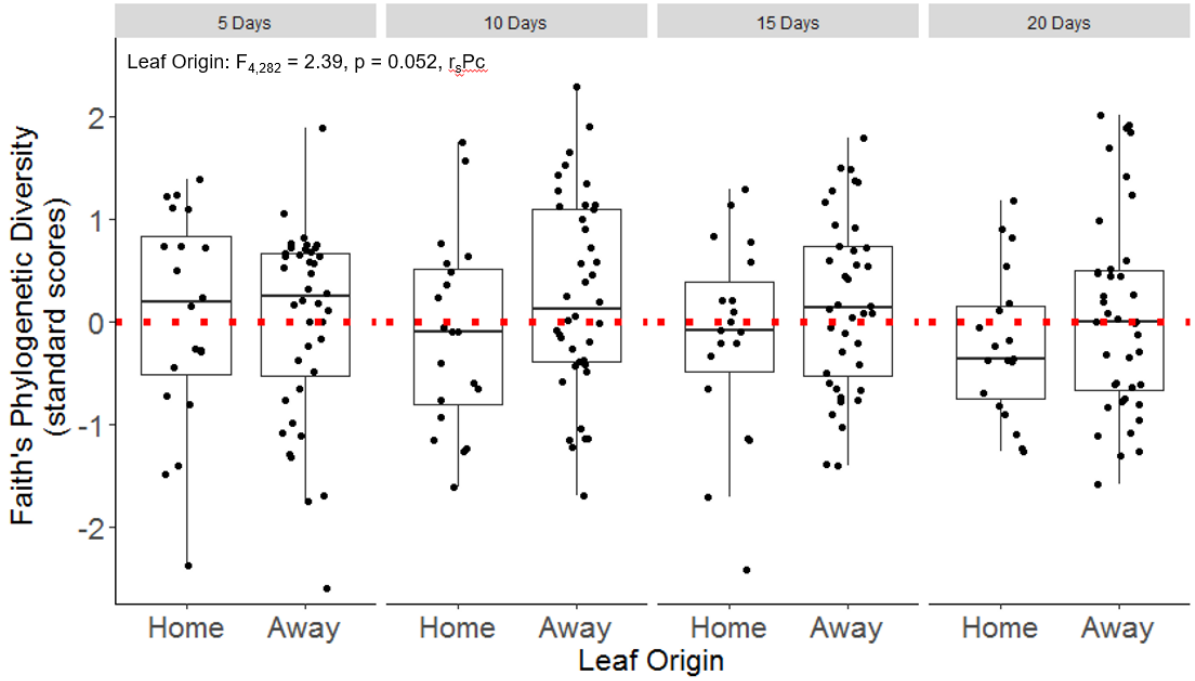


| | Df | SS | MS | F | Pr(>F) | $r_sP_C$ |
|---|---|---|---|---|---|---|
| Leaf Origin | 4 | 32527 | 8132 | 2.39 | 0.052 | < 0.01 |
| Day | 3 | 12890 | 4296 | | | |
| Tree | 19 | 96550 | 7426 | | | |
| Incubation Site | 3 | 20377987 | 6792662 | | | |
| Residuals | 282 | | | | | |

## ELECTRONIC SUPPLEMENTARY MATERIALS

**Fig. S7**. (A) Illustration of the subset of pathways in the 'Degradation of Aromatic Compounds' pathway that involve the 12 molecular functional terms that were identified as key differences between the bacterial communities inhabiting Home versus Away leaves using principal component analyses. See the PCA in Fig. 3C and panel (B) for further description of the 12 molecular functional terms. The corresponding table lists all the KEGG Ontology molecular functional terms included in the two Pathways included in our analyses using PICRUSt metagenome functional predictions. The 12 bold terms in the 'Degradation of Aromatic Compounds' pathway were key in distinguishing between bacterial communities inhabiting leaves of different leaf origin, while the 8 bold terms in the 'Metabolism of Starch & Sucrose' pathway are those that we studied further for their involvement in cellulose degradation. Further, (C) we report factor loadings for each of these 12 bolded terms in the 'Degradation of Aromatic Compounds' pathway that were used as variables in a principal component analysis that illustrates the distinct bacterial communities inhabiting Home versus Away leaves. Enzyme commission (EC) numbers provide a nomenclature reference and the Description column gives commonly used names.

(A)

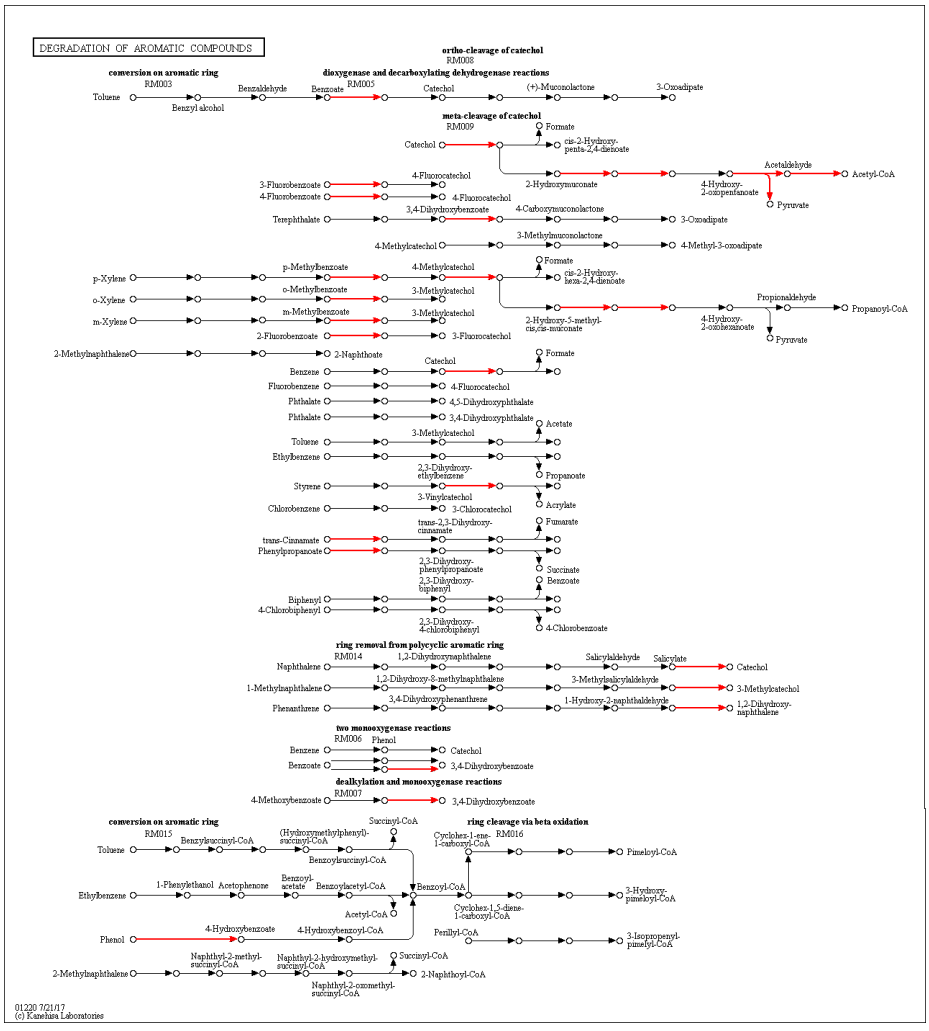

(B)

| Degradation of Aromatic Compounds | | Metabolism of Starch and Sucrose | |
|---|---|---|---|
| K00001 | K06912 | K02808 | K02438 |
| K00002 | K07104 | K02809 | K01200 |
| K00055 | K07535 | K02810 | K01176 |
| K00121 | K07536 | K01193 | K07405 |
| K00141 | K07537 | K00696 | K05343 |
| K00151 | K07538 | K07024 | K01177 |
| K00152 | K07539 | K00695 | K05992 |
| K00217 | K07540 | K12047 | K01208 |
| **K00446** | K08686 | K01187 | K01178 |
| K00448 | K08689 | K12316 | K21574 |
| **K00449** | K08690 | K12317 | K01182 |
| K00455 | K10217 | K01203 | K05988 |
| K00462 | K10219 | K20811 | K00705 |
| **K00480** | K10222 | K00692 | K16146 |
| **K00481** | K10616 | K18775 | K16147 |
| K00483 | K10617 | K01212 | K16148 |
| K00484 | K10619 | K05341 | K00691 |
| **K00529** | K10620 | K00689 | K01838 |
| K01053 | K10621 | K00690 | K02777 |
| K01055 | K10622 | K00963 | K02790 |
| K01607 | K10676 | K01513 | K02791 |
| **K01617** | K10700 | K00706 | K20107 |
| **K01666** | K10701 | K01199 | K20108 |
| **K01821** | K10702 | K19891 | K02749 |
| K01826 | K11947 | K19892 | K02750 |
| K01856 | K13953 | K19893 | K06896 |
| K01857 | K13954 | K01210 | K01232 |
| K02554 | K14519 | **K01188** | K00701 |
| **K03186** | K14578 | **K05349** | K01214 |
| K03268 | K14579 | **K05350** | K06044 |
| K03379 | K14580 | K00694 | K01236 |
| K03381 | K14581 | **K01179** | K13057 |
| K03464 | K14582 | **K19357** | K00697 |
| K04072 | K14583 | **K01225** | K01087 |
| **K04073** | K14584 | **K19668** | K16055 |
| K04105 | K14585 | **K00702** | K01194 |
| K04107 | K14727 | K02759 | K05342 |
| K04108 | K14748 | K02760 | K02817 |
| K04109 | K14749 | K02761 | K02818 |
| K04112 | K14750 | K01222 | K02819 |
| K04113 | K14751 | K01223 | K01226 |
| K04114 | | K00978 | K01835 |
| K04115 | | K00975 | K15778 |
| K05549 | | K18447 | K15779 |
| K05550 | | K00703 | K00844 |
| **K05708** | | K13679 | K12407 |
| K05709 | | K20812 | K00845 |
| K05710 | | K00693 | K01084 |
| K05711 | | K00750 | K11809 |
| K05712 | | K16150 | K01810 |
| K05713 | | K16153 | K06859 |
| K05714 | | K00700 | K13810 |
| K05783 | | K16149 | K15916 |
| **K05784** | | K00688 | K00847 |
| K05921 | | K01196 | |

(C)

| KEGG | PC1 | PC2 | EC # | Description |
|---|---|---|---|---|
| K00529 | 0.34061 | 0.03442 | 1.18.1.3 | 3-phenylpropionate/trans-cinnamate dioxygenase ferredoxin reductase component |
| K00449 | 0.24407 | -0.3266 | 1.13.11.3 | protocatechuate 3,4-dioxygenase, beta subunit |
| K00446 | 0.32109 | 0.30797 | 1.13.11.2 | catechol 2,3-dioxygenase |
| K00481 | 0.29366 | -0.3349 | 1.14.13.2 | p-hydroxybenzoate 3-monooxygenase |
| K00480 | 0.23182 | -0.4709 | 1.14.13.1 | salicylate hydroxylase |
| K05708 | 0.28502 | -0.3166 | 1.14.12.1 | 3-phenylpropionate/trans-cinnamate dioxygenase subunit alpha |
| K04073 | 0.30571 | 0.32959 | 1.2.1.10 | acetaldehyde dehydrogenase |
| K05784 | -0.1348 | 0.08582 | 1.18.1 | benzoate/toluate 1,2-dioxygenase reductase component |
| K03186 | 0.25631 | 0.33135 | 2.5.1.129 | flavin prenyltransferase |
| K01617 | 0.36156 | 0.12552 | 4.1.1.77 | 2-oxo-3-hexenedioate decarboxylase |
| K01666 | 0.32134 | 0.3047 | 4.1.3.39 | 4-hydroxy 2-oxovalerate aldolase |
| K01821 | 0.298 | -0.1697 | 5.3.2.6 | 4-oxalocrotonate tautomerase |

## ELECTRONIC SUPPLEMENTARY MATERIALS

**Fig. S8.** As supplementary to Fig. 1 of the main text, here we show the corresponding decomposition measures as non-standardized data points in which decomposition rates within an incubation site have not been adjusted to a μ = 0, s.d. = 1. Categories on the x-axis include from right to left 1.) trees growing immediately upstream of the incubation site and 2.) trees growing further upstream of that incubation site at the 'Away Site' on the same river, both of which are considered 'Home,' and then 3.) trees growing downstream of the incubation site at the 'Away Site' on the same river, 4) trees growing at the upstream site on the paired river, and 5.) trees growing at the downstream site on the paired river, all three of which are considered 'Away.' Note that all points are horizontally jittered to minimize overplotting. Also note that leaf mass remaining can be above 100% because leaves absorb excess water when submerged in rivers. See supplementary methods for details of laboratory experiment that was completed to determine a regression equation for converted submerged leaf weight to fresh leaf weight (fresh weight = 0.941(blotted-dry mass) – 0.00337 ($R^2$ = 0.983).

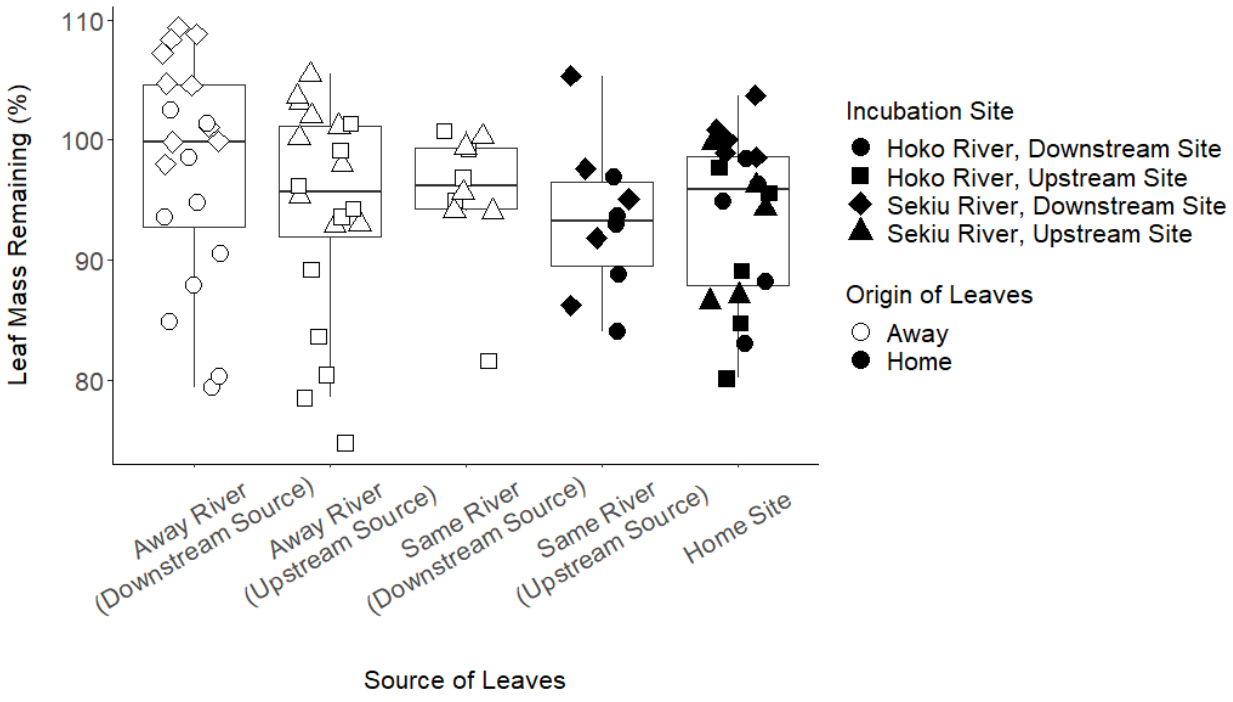

**ELECTRONIC SUPPLEMENTARY MATERIALS**

## Data Analysis Methods:

To determine whether leaves from locally-derived trees decomposed more rapidly than leaves sourced from non-local trees, we used ordered-ANOVA to account for our a priori prediction based on our prior studies that Home leaves decompose more quickly than Away leaves at each incubation site (Rice and Gaines 1994, Jackrel and Wootton 2014, Jackrel and Wootton 2015, Jackrel et al. 2016). Specifically, we used our ordered prediction to condense the original five-categories of leaf origin to a main contrast of Home versus Away. The Home group consisted of leaves from 1.) trees growing immediately upstream of the incubation site and 2.) trees growing further upstream of that incubation site at the 'Away Site' on the same river. Our Away group consisted of leaves from 3.) trees growing downstream of the incubation site at the 'Away Site' on the same river, 4.) trees growing at the upstream site on the paired river, and 5.) trees growing at the downstream site on the paired river. As aquatic leaf pack experiments result in initial and final leaf masses containing different moisture levels due to underwater leaf submergence, we previously performed experiments to determine the most accurate means of measuring grams of leaf mass loss rather than changes in water content (Jackrel and Wootton 2014). Leaf pack studies frequently use dried leaf litter from autumnal leaf fall in which leaves can be dried to a constant, precise initial mass before deployment. We aimed to find an accurate method appropriate for fresh, green leaves. Using dry weight is undesirable because drying leaves to obtain initial leaf mass fundamentally changes properties of fresh leaves in unnatural ways prior to experimental deployment. Therefore, to find an alternative method appropriate for fresh leaves, we collected 12 leaves from 19 red alder trees. We weighed groups of six leaves per tree at three stages: (1) freshly picked green leaves, (2) submerged in water for 17 days, and then blotted dry with paper towels, (3) oven-dried to a constant mass. The other six leaves per tree were oven-dried before and after submerging in water to estimate mass loss due to handling, leaching, and measurement error. The strongest correlation occurred between pre- and post-oven-dried leaves ($R^2 = 0.991$), which indicates minimal mass loss due to handling, measurement error, and/or leaching. However, the correlation between freshly picked leaf mass and the mass of leaves blotted dry with paper towels was nearly as strong ($R^2 = 0.983$). In contrast, the correlation between freshly picked leaf mass and oven dried leaf mass was appreciably weaker ($R^2 = 0.875$). Therefore, we used the relationship from the analysis of blotted dry leaves to back-calculate fresh mass of leaves following incubation in the rivers: fresh mass = 0.941(blotted-dry mass) – 0.00337 ($R^2 = 0.98$) (Jackrel and Wootton 2014). We also used an arcsine square root transformation on our decomposition rate data to meet assumptions of normality and homogeneity of variances. Our linear mixed effects model used leaf origin as a fixed effect and tree ID and incubation site as random effects. For the purposes of graphically representing our model results, we then converted percentage leaf mass lost data to z-scores that were standardized by incubation site. In practice, either using standard scores as our dependent variable or including incubation site as a fixed effect in the model yielded similar statistical results regarding our leaf origin treatment.

We analyzed our bacterial sequencing data using the QIIME pipeline (Caporaso et al. 2010). We classified operational taxonomic units (OTUs) from Illumina reads at the 97% similarity level using open reference-based clustering with uclust. We assigned a taxonomy using the RDP taxonomic assignment comparing the OTUs sequences against the Greengenes

database, version 13_8. Although the Greengenes database is smaller and less frequently updated than other frequently used databases, such as SILVA, Greengenes was preferable for our study because it is the only database that is compatible with the functional annotation tool PICRUSt, and is also the only database that provides in-depth taxonomic classification to the species level. We first determined which taxa varied over the course of succession from our leaf pack samples by asking whether collection day significantly predicted taxon relative abundance using analysis of variance with a multiple comparisons, false discovery rate correction (Benjamini and Hochberg 1995). Our model included three categorical variables (day, incubation site, leaf origin) and their interactions. We restricted this analysis to 91 OTUs that comprised at least 1% of the community in at least one of our samples, rather than averaging across our sample set, in order to include taxa that may comprise a sizable portion of the community in only a subset of samples. We identified taxa exhibiting consistent trends in relative population size across incubation sites as those taxa that either did not show a significant interaction between day and incubation site, or that showed the same directional trend for each site as determined visually with interaction plots. For those taxa showing consistent trends across incubation sites, we further categorized them as early, mid, or late successional taxa, defined as relative abundance that peaked on day 5, day 10 or 15, or day 20, respectively. We then highlighted taxa where successional patterns were contingent on leaf origin by noting those taxa with a significant interaction term between day and leaf origin. We also examined successional changes through time with principal coordinates analyses using the non-phylogenetically based Bray-Curtis distance metric, as well as the relative abundance-weighted and unweighted phylogenetically-based community distance metric, UNIFRAC (QIIME: principal_coordinates.py). We highlighted the top ten most abundant taxa that changed markedly across this successional gradient using biplot analyses that were superimposed in principal coordinate space (QIIME: make_emperor.py). We then measured changes in alpha diversity by day and by leaf origin using total OTU Number and Faith's Phylogenetic Diversity (QIIME: core_diversity_analyses). We used a mixed-effects linear regression model with our day treatment as a categorical fixed effect and incubation site and tree ID as random effects. We verified that the resulting model met assumptions of normality and homogeneity of variances. We then tested our main contrast that communities that inhabit Home versus Away leaves differed in alpha diversity using a mixed-effects linear regression models with leaf origin and day as our fixed effects and tree ID and incubation site as random effects. Our leaf origin treatment included all five categories as described above, and so we again incorporated our ordered a priori hypothesis that our Home groups would significantly differ in alpha diversity from our Away groups (Rice and Gaines 1994).

We predicted where the bacterial communities inhabiting our leaf packs originated using Bayesian SourceTracker models (Knights et al. 2011). We generated four site-specific models using a uniform prior by setting equal Dirichlet hyperparameters for our known source environments, including the riparian soil, terrestrial leaves, and the water column, and our unknown source environment (i.e., alpha1 = alpha2 = 0.001). Models for each incubation site included only the subset of riparian soil, water column, and leaf pack samples that were collected from or deployed at that site. The complete set of terrestrial leaf samples was used in each model because leaves from each study tree were deployed at each site. In addition to these four site-specific models, we also further subdivided the dataset to generate tree-specific models at each site in which for the leaf packs from a single tree we only consider the terrestrial leaves from that

tree as a potential source. We report only our four site-specific models because tree-specific models indicated similar proportional contributions of each source.

We next tested the effect of both succession (i.e. day) and our leaf origin treatment on the predicted gene content associated with different metabolic pathways of bacterial communities. We predicted metagenome functional content from our 16S survey data using the PICRUSt software package (Phylogenetic Investigation of Communities by Reconstruction of Unobserved States) (Langille et al. 2012). This pipeline uses ancestral-state reconstruction to predict the presence of gene families and then multiplies predicted functions by OTU relative abundances. To verify the accuracy of our functional predictions, we calculated Nearest Sequences Taxon Index for each sample. This is a relative-abundance weighted index that sums the phylogenetic distances for each OTU in a sample to the nearest relative with a sequenced genome and weights these OTU-specific measures by the frequency of the OTU in a sample (Langille et al. 2012). To identify specific molecular functions of interest we use the Kyoto Encyclopedia of Genes and Genomes (KEGG) Database to identify which specific molecular-level functional terms or KEGG terms are involved in certain functional pathways that we hypothesized were important for leaf degradation. We first tested whether bacterial communities differed in their functional capacity to degrade plant secondary metabolites using the KEGG Pathway: 'Degradation of Aromatic Compounds.' This pathway includes degradation reactions that we have inferred would be involved in the metabolism of two major classes of secondary metabolites in red alder, the polyphenol-based ellagitannins and the diarylheptanoids For example, this pathway includes reactions for the degradation of catechol, benzoates, trans cinnamate, and phenolic acids, which are all subunits of alder secondary metabolites.

We next derived a more general metric of the capacity of bacterial communities to degrade plant material. We used the 'Starch & Sucrose Metabolism,' pathway that includes enzymes involved in the degradation of cellulose, including endogluconase and cellulose 1,4-β-cellobiosidase. All KEGG Ontology Terms included in these two pathways at the time of download from < http://www.genome.jp/kegg/pathway.html> in October of 2017 are listed in Table S4. Within the Starch & Sucrose Metabolism pathway we also identified 8 KEGG Terms specifically involved in cellulose degradation that we refer to as the 'Degradation of Cellulose' pathway. For each pathway, we summed across all KEGG terms included in the pathway that were represented in our dataset to obtain a total measure of pathway function per sample. We refer to these new summary variables as the 'summed capacity' of bacterial communities to degrade aromatic compounds, the summed capacity to metabolize starch and sucrose, and the summed capacity to degrade cellulose.

We note that our dataset precludes us from testing whether variation in leaf chemistry drives variation in predicted gene content associated with different metabolic pathways. We have demonstrated that the secondary chemistry of alders can vary over short time scales in response to herbivore stress and/or nutrient availability (Jackrel and Morton, 2018). Therefore, although we have reported leaf chemistry data on the same trees used in the present study in Jackrel et al. 2016, it would be inaccurate to make inferences between bacteria that inhabited leaves in Summer 2013 with chemistry data analyzed from leaves collected in Summer 2012. Instead, we use our prior analyses to determine which metabolic pathways align best with the classes of secondary metabolites that predominate in alder trees growing at our study sites.

We tested whether functional capacities changed through succession (i.e., day) and by leaf origin. First, we tested for changes though succession with simple linear models of day as our continuous predictor variable and the summed function as our response variable. We also

tested whether individual KEGG Terms within the Degradation of Cellulose pathway changed significantly through succession using the same model structure, and a false-discovery rate correction for multiple comparisons. Second, we tested the effect of leaf origin on capacity to degrade aromatic compounds during day 5, because this was when this function was generally greatest. Similarly, we tested the effect of leaf origin on the capacity to metabolize starch and sucrose, as well as more specifically on the capacity to degrade cellulose, during day 20 when these functions were generally greatest. For these analyses we only used leaves for our categories that represented the strongest contrast and had the greatest sample sizes: leaves incubating at the Home Site on the Home River, versus leaves incubating at the Away River. We tested whether these same Home versus Away groups differed in the capacity of their bacterial communities to degrade aromatic compounds using a two-way ANOVA with treatment groups of leaf origin and Incubation Site. Because this result was significant, we then proceeded to run similar analyses testing whether leaf origin differed for each individual KEGG Ontology term in the Degradation of Aromatic Compounds pathway. Terms that were significant after false discovery rate correction were then used as variables in a principal component analyses to examine the distinct functional capacities of bacterial communities inhabiting leaves of Home versus Away origin.

Lastly, we tested whether the composition of the leaf bacterial community alone could predict the rate of leaf decomposition. We then asked whether adding these data describing the leaf bacterial community improved our original model of leaf decomposition that used leaf origin as the sole predictor variable. Our null model included random effects of day, incubation site, and tree ID. We used percentage leaf mass lost as our response variable and a mix of the following predictor variables: Faith's Phylogenetic Diversity as our measure of alpha diversity, summed capacity to degrade aromatic compounds, summed capacity to degrade cellulose, and our 5-category leaf origin treatment. We selected best fitting models by comparing AIC scores. We report marginal $R^2$ values for the best fitting mixed-effects models to describe variance explained by the fixed factors (Nakagawa and Schielzeth 2013). For the best fitting model, we report the F-statistic for each main effect, as well as the numerator and denominator degrees of freedom using the ANOVA function in R (R Core Team, 2017).

References:


Benjamini Y, Hochberg, Y. 1995. Controlling the false discovery rate: A practical and powerful approach to multiple testing. Journal of the Royal Statistical Society. Series B Methodological 57:289-300.

Jackrel SL, Morton, TC. 2018. Inducible phenotypic plasticity in plants regulates aquatic ecosystem functioning. Oecologia 186: 895-906.

Lundberg DS, Yourstone S, Mieczkowski P, Jones CD, Dang, JL. 2013. Practical innovations for high-throughput amplicon sequencing. Nature Methods 10:999-1002.

R Core Tream. 2017. R: A language and environment for statistical computing. R Foundation for Statistical Computing, Vienna, Australia. https://www.R-project.org/.

Rice WR, Gaines SD. 1994. The ordered-heterogeneity family of tests. Biometrics 50:746-752.

Nakagawa S, Schielzeth H. 2013. A general and simple method for obtaining $R^2$ from generalized linear mixed-effects models. Methods in Ecology and Evolution 4:133-142.